

Anomalous behavior of electric-field Fréedericksz transitions

Eugene C. Gartland, Jr.

Department of Mathematical Sciences, Kent State University, Kent, OH 44242, USA

ARTICLE HISTORY

Compiled September 13, 2024

ABSTRACT

Fréedericksz transitions in nematic liquid crystals are re-examined with a focus on differences between systems with magnetic fields and those with electric fields. A magnetic field can be treated as uniform in a liquid-crystal medium; while a nonuniform director field will in general cause nonuniformity of the local electric field as well. Despite these differences, the widely held view is that the formula for the threshold of local instability in an electric-field Fréedericksz transition can be obtained from that for the magnetic-field transition in the same geometry by simply replacing the magnetic parameters by their electric counterparts. However, it was shown in [Arakelyan, Karayan, and Chilingaryan, *Sov. Phys. Dokl.*, **29** (1984) 202–204] that in two of the six classical electric-field Fréedericksz transitions, the local-instability threshold should be *strictly greater* than that predicted by this magnetic-field analogy. Why this elevation of the threshold occurs is carefully examined, and a simple test to determine when it can happen is given. This “anomalous behavior” is not restricted to classical Fréedericksz transitions and is shown to be present in certain layered systems (planar cholesterics, smectic A) and in certain nematic systems that exhibit periodic instabilities.

KEYWORDS

Nematic liquid crystals; Frank free energy; Fréedericksz transitions; electric fields

1. Introduction

Fréedericksz transitions are the most basic instability in the study of liquid crystals. In simplest terms, a Fréedericksz transition occurs when an externally applied magnetic or electric field reaches a strength that is sufficient to distort the uniform orientational equilibrium state of a liquid-crystal sample, the ground-state configuration having been imposed by anchoring conditions on confining substrates. Different orientations of the liquid-crystal ground state and the external field give rise to different types of Fréedericksz transitions. This phenomenon has been studied for decades in a large number of variations and is discussed in all the standard texts—see [1–5], where references to the historical literature can also be found. Here we focus on differences that can occur between magnetic-field and electric-field Fréedericksz transitions with respect to *local instability thresholds*, differences that are little known and not well understood.

We consider the simplest liquid-crystal phase, an achiral uniaxial nematic, modeled at the macroscopic level in terms of the continuum theory of Oseen, Zocher, and Frank. The free energy of the system is expressed in terms of an integral functional of the nematic director \mathbf{n} , a unit-length vector field representing the average orientation of the distinguished axis of the anisometric molecules in a fluid element at a point. Intermolecular forces encourage local parallel alignment of \mathbf{n} . In the uniaxial nematic phase, the material is *transversely isotropic*, the magnetic and electric susceptibilities having one value for fields aligned parallel to \mathbf{n} and another value for fields perpendicular to it. If the anisotropy is *positive* (the susceptibility parallel to \mathbf{n} greater than that perpendicular to it), then the external field will exert a couple

on n encouraging it to align *parallel* to the external field; while if the anisotropy is *negative*, the field will encourage the director to orient *perpendicular* to the field.

Magnetic fields are influenced by the presence of a liquid-crystal medium. For the typical parameter values of such materials, however, this influence is negligible. Thus a magnetic field in a liquid crystal can be treated as a *uniform* external field. An electric field is influenced by a liquid-crystal medium as well but with a much stronger coupling—we make this more precise in the next section. The distinction between these two cases is discussed in [1, Sec. IV.1], [2, Sec. 3.4.1], [3, Sec. 3.3], [4, Sec. 4.1], [5, Sec. 2.3], and [6, 7]. Thus the equilibrium state of a liquid crystal subject to an electric field should be determined in a self-consistent way, with the director field and the electric field treated as *coupled* state variables. In general this coupling leads to *inhomogeneity* of the electric field and complicates the determination of equilibrium fields and the assessment of their local stability properties.

While the differences between magnetic fields and electric fields in liquid crystals have been appreciated for some time, the widely held view is that they only give rise to modest *quantitative* differences but not to *qualitative* differences in the context of instabilities such as Fréedericksz transitions. For example, in [1, Sec. IV.1] (referencing [8, 9]), [3, Sec. 3.3.1] (referencing [8]), and [5, Sec. 3.5], it is asserted that electric-field Fréedericksz thresholds can be obtained from the formulas for magnetic-field thresholds simply by substituting the electric parameters for the corresponding magnetic parameters. In fact, this was borne out in [9] (recounted in [1, Sec. IV.1]) and in [10] (recounted in [5, Sec. 3.5]) for the case of the electric-field splay-Fréedericksz transition, and this has contributed to the almost universal acceptance of this “magnetic-field analogy.”

Contrary to the above, in [6] (a paper that is not very well known) it was shown that both the electric-field bend-Fréedericksz transition with a positive dielectric anisotropy and the splay transition with a negative anisotropy have instability thresholds that are *strictly greater* than those predicted by simply replacing the magnetic parameters by their electric counterparts. We confirmed this result in [7] and further showed that this effect is more general and is also “one sided”: taking into account the coupling between the electric field and the director field can *elevate* an electric-field-induced instability threshold or leave the threshold *unchanged*, but it can *never lower* it. In [7] we also developed a simple criterion (based on problem geometry and field orientations) to identify situations in which such a threshold-elevating effect would take place. Details are provided in what follows.

The two Fréedericksz transitions mentioned above (the bend transition with a positive anisotropy and the splay transition with a negative anisotropy) are closely related in their modeling and are the only ones of the six classical electric-field transitions that exhibit this anomalous behavior—the other four transitions follow the magnetic-field analogy. The purpose of the present paper is to explain this and to illustrate how it fits into the framework of a more general theory of electric-field-induced instabilities (as developed in [7]). Circumstances that enable the electric-field transition to be *first order* emerge from the analysis as well. This work was motivated by results of experiments reported in [11, 12] and related numerical investigations presented in [13]. In addition to these *classical* Fréedericksz transitions, certain “generalized Fréedericksz transitions” exhibit this anomalous behavior—these include periodic instabilities in certain nematic systems and in some layered systems (planar cholesteric and smectic-A films)—and these are discussed as well.

The paper is organized as follows. In Section 2, free energies that can be used to model the magnetic-field and electric-field Fréedericksz transitions are given, and the differences between them are discussed. The classical magnetic-field transitions are reviewed in Section 3, with the local stability of equilibrium states studied from a variational point of view. The modeling of the analogous electric-field transitions is considered in Section 4, pointing out the differences among the cases that result from the different geometries. In Section 5, the electric-field bend-Fréedericksz transition with positive dielectric anisotropy is carefully analyzed, and the formula for the elevated local-instability threshold predicted in [6] is re-derived using a perturbation expansion. A necessary condition for the local stability of an equilibrium director field and coupled electric field in a general setting is given in Section 6. This condition provides a “litmus test” for when an instability threshold will be altered and also illustrates why a threshold

can only be elevated, not lowered. Applications to both classical and generalized Fréedericksz transitions illustrating the utility of this test are discussed. In Section 7, results of experiments reported in [11] are shown to be in qualitative agreement with predictions here. The main findings are summarized in the concluding Section 8.

2. Free energies: electric fields versus magnetic fields

Equilibrium states of the systems we study are characterized as stationary points of appropriate free-energy functionals. For magnetic fields generated by current-stabilized electromagnets or electric fields produced by electrodes held at constant potential, the free energies have the general forms

$$\mathcal{F}_H = \int_{\Omega} \left(W_e - \frac{1}{2} \mathbf{B} \cdot \mathbf{H} \right) dV, \quad \mathcal{F}_E = \int_{\Omega} \left(W_e - \frac{1}{2} \mathbf{D} \cdot \mathbf{E} \right) dV,$$

where Ω is the region occupied by the liquid crystal. Here \mathbf{B} is the magnetic induction, \mathbf{H} the magnetic field, \mathbf{D} the electric displacement, \mathbf{E} the electric field, and W_e denotes the distortional elasticity, which can be written in the form of the classical Frank formula

$$W_e = \frac{K_1}{2} (\operatorname{div} \mathbf{n})^2 + \frac{K_2}{2} (\mathbf{n} \cdot \operatorname{curl} \mathbf{n})^2 + \frac{K_3}{2} |\mathbf{n} \times \operatorname{curl} \mathbf{n}|^2 + K_{24} [\operatorname{tr}(\nabla \mathbf{n})^2 - (\operatorname{div} \mathbf{n})^2]. \quad (1)$$

See [4, Sec. 3.2] or [5, Sec. 2.2]. The elastic constants K_1 , K_2 , K_3 , and K_{24} are material and temperature dependent. For a transversely isotropic medium in the linear regime, the magnetic quantities can be taken in the form

$$\mathbf{B} = \mu_0 (\mathbf{M} + \mathbf{H}), \quad \mathbf{M} = \boldsymbol{\chi}(\mathbf{n}) \mathbf{H}, \quad \boldsymbol{\chi} = \chi_{\perp} \mathbf{I} + \Delta \chi (\mathbf{n} \otimes \mathbf{n}), \quad \Delta \chi := \chi_{\parallel} - \chi_{\perp},$$

where μ_0 is the free-space permeability, \mathbf{M} the magnetization, $\boldsymbol{\chi}$ the susceptibility tensor, and χ_{\parallel} and χ_{\perp} the susceptibilities parallel to \mathbf{n} and perpendicular to \mathbf{n} (with values in the range $|\chi_{\perp}|, |\chi_{\parallel}| \approx 10^{-6} - 10^{-5}$ in SI units for liquid-crystal materials, [3, Sec. 3.2.1]). Using these expressions, the equations of magnetostatics in the absence of any current density ($\operatorname{curl} \mathbf{H} = \mathbf{0}$, $\operatorname{div} \mathbf{B} = 0$) guarantee the existence of a magnetic scalar potential φ_m that must satisfy

$$\Delta \varphi_m + \frac{\Delta \chi}{1 + \chi_{\perp}} \operatorname{div} [(\nabla \varphi_m \cdot \mathbf{n}) \mathbf{n}] = 0, \quad \mathbf{H} = -\nabla \varphi_m.$$

For typical liquid crystals, $\Delta \chi / (1 + \chi_{\perp}) \approx 10^{-6}$ (see [3, Sec. 3.2.1]), and the term involving \mathbf{n} above is negligible—the magnetic field is uninfluenced by the director field to a high degree of approximation.

The electric quantities for a medium such as ours have forms that are similar to those for the magnetic quantities, though they are usually expressed in slightly different notation:

$$\mathbf{D} = \boldsymbol{\varepsilon}(\mathbf{n}) \mathbf{E}, \quad \boldsymbol{\varepsilon} = \varepsilon_0 [\varepsilon_{\perp} \mathbf{I} + \varepsilon_a (\mathbf{n} \otimes \mathbf{n})], \quad \varepsilon_a := \varepsilon_{\parallel} - \varepsilon_{\perp}, \quad (2)$$

where ε_0 is the free-space permittivity, $\boldsymbol{\varepsilon}$ the dielectric tensor, and ε_{\parallel} and ε_{\perp} the permittivities parallel to \mathbf{n} and perpendicular to \mathbf{n} . Assuming there is no distribution of free charge, the equations of electrostatics ($\operatorname{curl} \mathbf{E} = \mathbf{0}$, $\operatorname{div} \mathbf{D} = 0$) guarantee the existence of an electric potential φ that must satisfy (cf., [4, Eqn. (4.12)])

$$\Delta \varphi + \frac{\varepsilon_a}{\varepsilon_{\perp}} \operatorname{div} [(\nabla \varphi \cdot \mathbf{n}) \mathbf{n}] = 0, \quad \mathbf{E} = -\nabla \varphi. \quad (3)$$

The difference here is that the factor $\varepsilon_a/\varepsilon_\perp$ is $O(1)$ for typical liquid-crystal materials, and the term involving \mathbf{n} above cannot be ignored—the liquid-crystal medium has a non-negligible influence on the local electric field. As an example, the values of these different factors for the material 5CB near 26°C are given by

$$\frac{\Delta\chi}{1 + \chi_\perp} = 1.43 \times 10^{-6}, \quad \frac{\varepsilon_a}{\varepsilon_\perp} = 1.64,$$

using data given in [5, Table D.3].

While there are other ways to see this, the above makes it clear that for the systems that are of interest to us, the magnetic field can be treated as uniform, unaffected by the medium (a true external field), while the electric field should be viewed as coupled to the director field. These modeling assumptions lead to

$$\mathbf{B} \cdot \mathbf{H} = \chi_a(\mathbf{H} \cdot \mathbf{n})^2 + \text{const}, \quad \chi_a := \mu_0 \Delta\chi, \quad \mathbf{D} \cdot \mathbf{E} = \varepsilon(\mathbf{n}) \nabla\varphi \cdot \nabla\varphi,$$

and the free energies for the magnetic field and electric field cases have the forms

$$\begin{aligned} \mathcal{F}_H[\mathbf{n}] &= \int_{\Omega} \left[W_e(\mathbf{n}, \nabla\mathbf{n}) - \frac{1}{2} \chi_a (\mathbf{H} \cdot \mathbf{n})^2 \right] dV, \\ \mathcal{F}_E[\mathbf{n}, \varphi] &= \int_{\Omega} \left[W_e(\mathbf{n}, \nabla\mathbf{n}) - \frac{1}{2} \varepsilon(\mathbf{n}) \nabla\varphi \cdot \nabla\varphi \right] dV. \end{aligned} \tag{4}$$

Both χ_a and ε_a can be *positive* or *negative*.

Globally stable solutions for a system with a magnetic field satisfy

$$\mathcal{F}_H[\mathbf{n}^*] = \min_{\mathbf{n}} \mathcal{F}[\mathbf{n}],$$

subject to regularity assumptions, appropriate boundary conditions, and the pointwise constraint $|\mathbf{n}| = 1$. The dielectric tensor ε is real, symmetric, and *positive definite*; so for a system with an electric field, globally stable solution pairs are characterized by

$$\mathcal{F}_E[\mathbf{n}^*, \varphi^*] = \min_{\mathbf{n}} \max_{\varphi} \mathcal{F}_E[\mathbf{n}, \varphi],$$

subject to appropriate auxiliary conditions on both \mathbf{n} and φ . We note that this “minimax” problem can be written in an equivalent way as a constrained minimization problem:

$$\mathcal{F}_E[\mathbf{n}^*, \varphi^*] = \min_{\mathbf{n}} \mathcal{F}_E[\mathbf{n}, \varphi], \quad \text{subject to } \text{div}[\varepsilon(\mathbf{n}) \nabla\varphi] = 0.$$

The constraint, which results from the maximization of \mathcal{F}_E with respect to φ with a fixed director field \mathbf{n} , is equivalent to the electrostatic equation $\text{div} \mathbf{D} = 0$ (another way of writing (3)). In this setting, the electric potential field can be thought of as “slaved” to the director field, uniquely determined for any given \mathbf{n} on Ω . The problem for the globally stable solution in the presence of an electric field can then be formulated in various ways: as a minimax problem for \mathbf{n} and φ , as a constrained minimization problem for \mathbf{n} (with φ satisfying a partial differential equation constraint), or in terms of a “least free energy principle” (in the sense that a globally stable solution pair $(\mathbf{n}^*, \varphi^*)$ has the *lowest* free energy among all *equilibrium pairs*).

Most of the formulations in this section can be found in standard references. The Frank elastic model is well established, well studied, and well presented in [2–5], as are the magnetic-field Fréedericksz transitions. Some references take the approach that treating the electric field in a liquid-crystal medium as uniform is a reasonable approximation, based upon the assumption that $\varepsilon_a/\varepsilon_\perp \ll 1$. This is how it is viewed in [4, Sec. 4.1], sometimes referred to in the literature as “the magnetic approximation.” As we have seen, this assumption is not always valid. Other

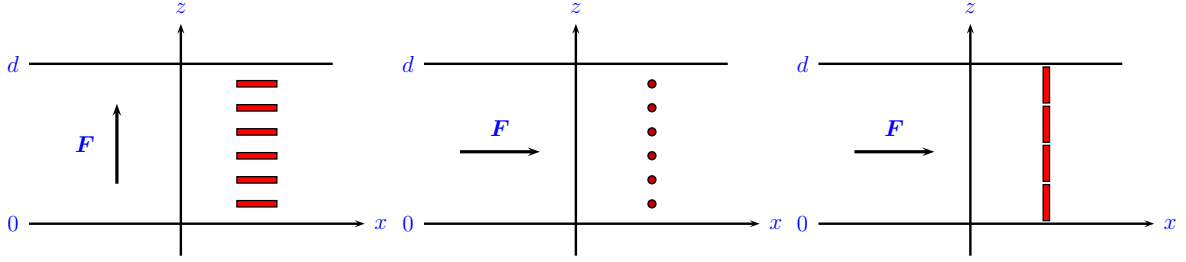


Figure 1. Geometries of the three classical Fréedericksz transitions in *magnetic* or *electric* fields ($\mathbf{F} = \mathbf{H}$ or $\mathbf{F} = \mathbf{E}$) for a material with a *positive* anisotropy ($\chi_a > 0$ or $\varepsilon_a > 0$): “splay” (left, director constrained to x - z tilt plane), “twist” (center, director constrained to x - y twist plane), “bend” (right, director constrained to x - z tilt plane).

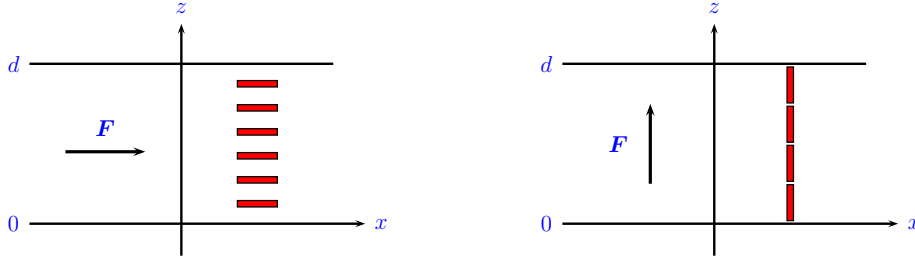


Figure 2. Geometries of classical Fréedericksz transitions in *magnetic* or *electric* fields ($\mathbf{F} = \mathbf{H}$ or $\mathbf{F} = \mathbf{E}$) for materials of *negative* anisotropy ($\chi_a < 0$ or $\varepsilon_a < 0$): “splay” (left, director constrained to x - z tilt plane), “twist” (left, director constrained to x - y twist plane), “bend” (right, director constrained to x - z tilt plane).

references acknowledge that a nonuniform director field can cause a nonuniform electric field, but they maintain that Fréedericksz thresholds are not affected by this. This is the case in [1, Sec. IV.1], [3, Sec. 3.3.1], and [5, Sec. 3.5]. Only in [2, Sec. 3.4.1] does one find mention of the fact that the analogy between electric and magnetic fields breaks down “when the dielectric anisotropy is very large,” allowing for a first-order electric-field Fréedericksz transition “in certain geometries” (referencing [6, 11, 14]). Nothing is said there about the formulas for the local instability thresholds. We note that having a large dielectric anisotropy is a desirable feature of a material for most applications of liquid crystals.

3. Magnetic-field Fréedericksz transitions

We summarize results for the classical magnetic-field Fréedericksz transitions from a variational point of view, as found, for example, in [4, 5]. There are six cases: three corresponding to materials with positive magnetic anisotropy ($\chi_a > 0$), three for materials with $\chi_a < 0$. The geometries of the classical transitions (with either magnetic or electric fields) are depicted in Figures 1 and 2 for reference. These illustrate the orientations of the ground-state director fields and the external magnetic or electric fields, as well as the coordinate system to be used here. The anchoring conditions are assumed to be infinitely strong and the lateral dimensions sufficiently large compared to the cell gap d such that the director field can be assumed to be uniform in those directions (a function of z only). In each case, the distortion of the director field is assumed to be restricted to a plane: the x - z tilt plane for the splay and bend transitions, the x - y twist plane for the twist transitions. The restriction of the director distortion to a plane is a bit of an idealization, as some additional mechanism (such as an additional external field) could be required to enforce this in some cases.

By virtue of the fact that the director field is assumed to be planar in each geometry, \mathbf{n} can be represented in terms of a single tilt or twist angle, and such a representation is convenient in analyzing the classical Fréedericksz transitions. For more general liquid-crystal systems (and for the more general theory of field-induced instabilities developed in [7]), the vector representation of \mathbf{n} is advantageous. An equilibrium director field for a system such as ours governed by a free

energy \mathcal{F}_H of the form in (4) can be characterized as a solution of a system of Euler-Lagrange equations

$$-\operatorname{div}\left(\frac{\partial W_e}{\partial \nabla \mathbf{n}}\right) + \frac{\partial W_e}{\partial \mathbf{n}} = \lambda \mathbf{n} + \chi_a (\mathbf{H} \cdot \mathbf{n}) \mathbf{H}, \text{ in } \Omega,$$

subject to appropriate boundary conditions and the unit-length constraint $|\mathbf{n}| = 1$ (which must hold at each point in the domain Ω). A certain amount of regularity of \mathbf{n} is also assumed. The scalar field λ is a Lagrange-multiplier field associated with the unit-length constraint and is given by

$$\lambda = \left[-\operatorname{div}\left(\frac{\partial W_e}{\partial \nabla \mathbf{n}}\right) + \frac{\partial W_e}{\partial \mathbf{n}} \right] \cdot \mathbf{n} - \chi_a (\mathbf{H} \cdot \mathbf{n})^2,$$

with the expression above evaluated at the equilibrium director field. Note that λ is a scalar *field*; though in simple cases, it could be a constant. In particular, λ is constant for the ground states of all six of the basic Fréedericksz geometries, and $\lambda = 0$ for the three transitions with $\chi_a > 0$ —this follows from the vanishing of the bracketed term above for any spatially uniform vector field \mathbf{n} (with W_e as in (1)) and the fact that $\mathbf{H} \cdot \mathbf{n} = 0$ for the geometries with $\chi_a > 0$ (those in Figure 1). These conditions hold as well for the analogous electric-field cases.

For an equilibrium director field \mathbf{n}_0 to be *locally stable* (metastable) in general, its free energy should lie at the bottom of a well on the free-energy surface. This can be determined by evaluating the free energy on admissible director fields close to \mathbf{n}_0 . Such fields can be produced, for example, in the form

$$\mathbf{n}_\epsilon = \frac{\mathbf{n}_0 + \epsilon \mathbf{v}}{|\mathbf{n}_0 + \epsilon \mathbf{v}|},$$

as is used in [4, Sec. 3.5] and [15]. The fields \mathbf{n}_ϵ are normalized so that $|\mathbf{n}_\epsilon| = 1$ on Ω (for any \mathbf{v} , with $|\epsilon|$ sufficiently small). The perturbative field \mathbf{v} must also be such that \mathbf{n}_ϵ satisfies the boundary conditions that \mathbf{n} must satisfy. In a general setting, these conditions could include strong anchoring, weak anchoring, periodic boundary conditions, etc., and an account along those lines is given in [7]. Here, for simplicity, we assume that \mathbf{n} must satisfy *strong anchoring* conditions on the entire boundary of Ω (denoted $\partial\Omega$). Thus for \mathbf{n}_ϵ to be admissible, \mathbf{v} must *vanish* on $\partial\Omega$. Expanding for small ϵ gives

$$\mathbf{n}_\epsilon = \mathbf{n}_0 + \epsilon \mathbf{u} + O(\epsilon^2), \quad \mathbf{u} = \mathbf{P}(\mathbf{n}_0) \mathbf{v}, \quad \mathbf{P}(\mathbf{n}) := \mathbf{I} - \mathbf{n} \otimes \mathbf{n}. \quad (5)$$

The linear operator $\mathbf{P}(\mathbf{n})$ gives the projection transverse to \mathbf{n} : $\mathbf{P}(\mathbf{n}) \mathbf{v} \perp \mathbf{n}$ (cf., [4, Sec. 3.2]). If λ_0 is the Lagrange multiplier field associated with \mathbf{n}_0 , then the expansion of the free energy of \mathbf{n}_ϵ can be expressed

$$\mathcal{F}_H[\mathbf{n}_\epsilon] = \mathcal{F}_H[\mathbf{n}_0] + \frac{1}{2} \epsilon^2 \left[\delta^2 \mathcal{F}_H[\mathbf{n}_0](\mathbf{u}) - \int_{\Omega} \lambda_0 |\mathbf{u}|^2 dV \right] + o(\epsilon^2), \quad (6)$$

with $\mathbf{u} = \mathbf{P}(\mathbf{n}_0) \mathbf{v}$ as above. Here $\delta^2 \mathcal{F}_H$ denotes the *second variation* of the functional \mathcal{F}_H and has the form

$$\delta^2 \mathcal{F}_H[\mathbf{n}](\mathbf{v}) = \int_{\Omega} \left(\frac{\partial^2 W}{\partial n_i \partial n_k} v_i v_k + 2 \frac{\partial^2 W}{\partial n_i \partial n_{k,l}} v_i v_{k,l} + \frac{\partial^2 W}{\partial n_{i,j} \partial n_{k,l}} v_{i,j} v_{k,l} \right) dV, \\ W = W_e - \frac{1}{2} \chi_a (\mathbf{H} \cdot \mathbf{n})^2.$$

A derivation of (6) can be found in [7]. A term of first order in ϵ is not present in (6) because of the equilibrium conditions satisfied by \mathbf{n}_0 and λ_0 . The integral with the Lagrange-multiplier field

λ_0 compensates for the curvature of the constraint manifold $|\mathbf{n}_0| = 1$, which the perturbation \mathbf{u} enforces only to first order. The necessary condition for local stability of the equilibrium director field \mathbf{n}_0 , with associated Lagrange-multiplier field λ_0 , can then be expressed

$$\delta^2 \mathcal{F}_H[\mathbf{n}_0](\mathbf{u}) - \int_{\Omega} \lambda_0 |\mathbf{u}|^2 dV \geq 0, \quad (7)$$

and this must hold for all smooth test fields \mathbf{u} that are *transverse* to \mathbf{n}_0 ($\mathbf{n}_0 \cdot \mathbf{u} = 0$ on Ω) and *vanish* on the boundary $\partial\Omega$. This form of local stability assessment follows the approaches of [15] and [16].

As an illustration, consider the case of the splay-Fréedericksz transition with $\chi_a < 0$ (Figure 2 left). For this geometry,

$$\mathbf{n} = n_x(z)\mathbf{e}_x + n_z(z)\mathbf{e}_z,$$

the free energy (per unit cross-sectional area) has the form

$$\mathcal{F}_H[\mathbf{n}] = \frac{1}{2} \int_0^d (K_1 n_{z,z}^2 + K_3 n_{x,z}^2 - \chi_a H^2 n_x^2) dz,$$

and the equilibrium Euler-Lagrange system is given by

$$\begin{aligned} K_3 n_{x,zz} + (\chi_a H^2 + \lambda) n_x &= 0, & K_1 n_{z,zz} + \lambda n_z &= 0, & n_x^2 + n_z^2 &= 1, & 0 < z < d, \\ n_x(0) = n_x(d) &= 1, & n_z(0) = n_z(d) &= 0. \end{aligned}$$

The ground-state equilibrium solution of the above is given by

$$\mathbf{n}_0 = \mathbf{e}_x \quad (n_x = 1, n_z = 0), \quad \lambda_0 = -\chi_a H^2.$$

Boundary conditions with $n_x = -1$ and a ground state of $\mathbf{n}_0 = -\mathbf{e}_x$ would work equally well. Test fields \mathbf{u} in (7) must here be x - z planar and orthogonal to \mathbf{n}_0 on $0 < z < d$, and they must vanish at $z = 0$ and $z = d$. Thus they must be of the form

$$\mathbf{u} = w(z)\mathbf{e}_z, \quad w(0) = w(d) = 0.$$

The stability condition (7) then becomes

$$\delta^2 \mathcal{F}_H[\mathbf{n}_0](\mathbf{u}) - \int_0^d \lambda_0 |\mathbf{u}|^2 dz = K_1 \int_0^d w_{,z}^2 dz + \chi_a H^2 \int_0^d w^2 dz \geq 0,$$

which implies

$$-\frac{\chi_a H^2}{K_1} \leq \frac{\int_0^d w_{,z}^2 dz}{\int_0^d w^2 dz},$$

and this must hold for all smooth functions w that vanish at $z = 0$ and $z = d$. The minimum value of the expression on the right-hand side above over all such functions is given by

$$\min_{w(0)=w(d)=0} \frac{\int_0^d w_{,z}^2 dz}{\int_0^d w^2 dz} = \frac{\pi^2}{d^2}, \quad \text{attained by } w = \sin \frac{\pi z}{d}. \quad (8)$$

This can most readily be seen by using a modal expansion $w = \sum b_n \sin(n\pi z/d)$. The minimal value and attaining function above represent the minimum eigenvalue and associated eigenfunction of the eigenvalue problem

$$\frac{d^2 w}{dz^2} + \lambda w = 0, \quad w(0) = w(d) = 0.$$

It follows that in order for the ground state director field $\mathbf{n}_0 = \pm \mathbf{e}_x$ to be locally stable, the strength of the magnetic field must satisfy

$$H \leq \frac{\pi}{d} \sqrt{\frac{K_1}{-\chi_a}},$$

which is the correct instability threshold.

As modeled above, the local stability assessments for all six magnetic-field Fréedericksz transitions reduce to similar inequalities and ultimately rest upon the minimum-eigenvalue formula (8), giving the classical threshold formulas for the splay, twist, and bend transitions (valid for both $\chi_a > 0$ and $\chi_a < 0$):

$$H_c = \frac{\pi}{d} \sqrt{\frac{K_i}{|\chi_a|}}, \quad i = 1, 2, 3.$$

See [1, Sec. IV.1], [2, Sec. 3.4.1], [3, Sec. 3.2.3], [4, Sec. 4.2], [5, Sec. 3.4.1]. Rather than appeal to a general characterization of stability as in (7), most references analyze individual Fréedericksz transitions by direct consideration of appropriate free energies (expressed in terms of angle representations of \mathbf{n}), using first integrals obtained from the associated Euler-Lagrange equations. The textbook analyses also go a bit further and show that the classical magnetic-field Fréedericksz transitions are always *second order*, information that is not provided by (7). The advantage of (6) and (7) for our purposes is the way that they generalize to electric-field-induced instabilities, which are to follow. The example discussed above also illustrates the role that the Lagrange-multiplier field associated with an equilibrium director field can play in the assessment of the local stability of that director field.

4. Models of electric-field Fréedericksz transitions

Before discussing the characterization of local stability for equilibria with electric fields (generalizing (6) and (7)), we first illustrate the anomalous behavior of one of these transitions by direct analysis of its Euler-Lagrange equations. For now we consider only materials with $\varepsilon_a > 0$ —results for materials with $\varepsilon_a < 0$ can be obtained directly from these by simple substitutions of parameters. Thus we consider the three classical Fréedericksz geometries in Figure 1, but with electric fields instead of magnetic fields. The electric fields are created by electrodes, which in the case of the splay geometry (Figure 1 left) are on the top and bottom of the cell. For the twist and bend geometries (Figure 1 center, right), the electric field needs to be in the plane of the film, and so the electrodes must be placed on the left and right ends (across the wide dimension of the cell). We refer to the first case as “cross plane” and the latter cases as “in plane.” The two cases require somewhat different handling.

4.1. Cross-plane electric field

The electric-field splay-Fréedericksz transition was analyzed in [9] and [10] taking into account the coupling between the director field and the electric field. The electric field is confined to

the cell, with a potential difference V between the top and bottom electrodes. By assumption, $\mathbf{n} = n_x(z)\mathbf{e}_x + n_z(z)\mathbf{e}_z$ and $\varphi = \varphi(z)$. The relations $\mathbf{E} = -\nabla\varphi$ and $\text{div } \mathbf{D} = 0$ then give

$$\mathbf{E} = -\varphi_{,z}\mathbf{e}_z, \quad D_z = \text{const.}$$

Using these together with $\varphi(d) - \varphi(0) = V$, one can deduce the constant value of D_z and a non-local expression for \mathbf{E} in terms of \mathbf{n} (cf., [5, Eqns. (3.220) and (3.221)]):

$$D_z = -\varepsilon_0 V \left[\int_0^d \frac{dz}{\varepsilon_\perp n_x^2 + \varepsilon_\parallel n_z^2} \right]^{-1}, \quad \mathbf{E} = -V \left[\int_0^d \frac{dz}{\varepsilon_\perp n_x^2 + \varepsilon_\parallel n_z^2} \right]^{-1} \frac{1}{\varepsilon_\perp n_x^2 + \varepsilon_\parallel n_z^2} \mathbf{e}_z. \quad (9)$$

These enable one to write the free energy \mathcal{F}_E for this system in the form of a *reduced* functional of \mathbf{n} only:

$$\mathcal{F}[\mathbf{n}] = \frac{1}{2} \int_0^d (K_1 n_{z,z}^2 + K_3 n_{x,z}^2) dz - \frac{1}{2} \varepsilon_0 V^2 \left[\int_0^d \frac{dz}{\varepsilon_\perp n_x^2 + \varepsilon_\parallel n_z^2} \right]^{-1}. \quad (10)$$

The analyses of [9] and [10] were based upon studies of this functional and concluded that the critical voltage at which the uniform horizontal ground state of the director field becomes unstable is given by

$$V_c = \pi \sqrt{\frac{K_1}{\varepsilon_0 \varepsilon_a}}$$

and that the transition is *second order* for any $K_1, K_3 > 0$ and $\varepsilon_\parallel > \varepsilon_\perp > 0$. This instability follows the magnetic-field analogy:

$$E_c = \frac{V_c}{d} = \frac{\pi}{d} \sqrt{\frac{K_1}{\varepsilon_0 \varepsilon_a}} \leftrightarrow H_c = \frac{\pi}{d} \sqrt{\frac{K_1}{\chi_a}}.$$

The same results can be obtained by analyzing the free energy modeled as a functional of *both* \mathbf{n} and φ , which follows from the expression for \mathcal{F}_E in (4):

$$\mathcal{F}[\mathbf{n}, \varphi] = \frac{1}{2} \int_0^d [K_1 n_{z,z}^2 + K_3 n_{x,z}^2 - \varepsilon_0 (\varepsilon_\perp n_x^2 + \varepsilon_\parallel n_z^2) \varphi_{,z}^2] dz.$$

While this will now lead to a *coupled* set of equilibrium equations for \mathbf{n} and φ , the model has the advantage of being *local*, whereas the Euler-Lagrange equations associated with (10) above are of integro-differential type (cf., [5, Eqn. (3.226)]).

4.2. In-plane electric field

The electric-field twist and bend geometries both involve an electric field oriented in the plane of the film. This is an awkward geometry for experiments (electrodes on the wide ends of the cell), as well as for modeling (the electric field extending above and below the cell). Assuming as before that the cell gap is small compared to the lateral dimensions, boundary-layer theory suggests that the director field and electric field can be well approximated by “outer solutions” of the form $\mathbf{n} = \mathbf{n}(z)$ and $\mathbf{E} = \mathbf{E}(z)$ throughout most of the region plus boundary-layer corrections, the influence of which is significant only in narrow regions adjacent to the lateral boundaries. We shall thus model the systems with in-plane electric fields in terms of the *outer solutions* in this asymptotic regime, as was also done in [6, 11, 17]. This modeling assumption was validated to a degree by numerical experiments in [13, §4.3].

We assume a simple experimental setup, with tall electrodes on the left and right ends and with the regions above and below the cell consisting of stratified layers of homogeneous materials (alignment layers, polarizers, glass substrates, air, etc.), all with horizontal interfaces. This is the type of system that was used in the experiments reported in [11, 12]. Other experimental setups are possible (interdigitated electrodes, electrode strips as spacers), but it does not appear that they produce as uniform an electric field in the sample. Utilizing the assumptions $\mathbf{n} = \mathbf{n}(z)$ and $\mathbf{E} = \mathbf{E}(z)$ in the basic electrostatic equations $\text{curl } \mathbf{E} = \mathbf{0}$ and $\text{div } \mathbf{D} = 0$, together with *interface conditions* (E_x, E_y, D_z continuous) and *far-field conditions* as $z \rightarrow \pm\infty$ ($E_x = E_0, E_y = 0, D_z = 0$), one obtains an expression for the electric field that is valid throughout the entire region between the electrodes (inside the liquid-crystal cell, as well as in the extended regions above and below it):

$$\mathbf{E} = E_0 \mathbf{e}_x + E_z(z) \mathbf{e}_z, \quad E_0 := -V/l,$$

with $E_z = 0$ outside $0 \leq z \leq d$. Here $E_0 \mathbf{e}_x$ is the uniform electric field that one would have if there were no inhomogeneity in the medium between the electrodes, with V the potential difference between the electrodes and l the distance separating them.

Using the above expression for \mathbf{E} in the relation $D_z = 0$ (with \mathbf{D} as in (2)) gives

$$[\varepsilon_{\perp}(n_x^2 + n_y^2) + \varepsilon_{\parallel} n_z^2] E_z + \varepsilon_a n_x n_z E_0 = 0,$$

which can be solved for E_z in $0 < z < d$ in both the twist and bend cases: in the *twist* case,

$$\mathbf{n} = n_x \mathbf{e}_x + n_y \mathbf{e}_y \Rightarrow E_z = 0, \quad (11a)$$

in the *bend* case,

$$\mathbf{n} = n_x \mathbf{e}_x + n_z \mathbf{e}_z \Rightarrow E_z = -\varepsilon_a E_0 \frac{n_x n_z}{\varepsilon_{\perp} n_x^2 + \varepsilon_{\parallel} n_z^2}. \quad (11b)$$

It can be shown that the expressions for the electric field given above are precisely what one obtains if one formulates the full coupled system for the director field \mathbf{n} and electric potential φ (as functions of x and z), rescales introducing the small parameter $\eta := d/l$ (where d is the cell gap and l the distance between the electrodes), forms the problems for the outer solutions \mathbf{n} and φ (by setting $\eta = 0$), and solves the resulting problem for φ in terms of \mathbf{n} . The expression for E_z in the bend case in (11b) is as found in [6].

Using the expressions for \mathbf{n} and \mathbf{E} in (11a) and (11b) above, one can write the electric-field free energy \mathcal{F}_E in (4) for the twist and bend cases in the following forms:

$$\mathcal{F}[\mathbf{n}] = \frac{1}{2} \int_0^d [K_2(n_x n_{y,z} - n_y n_{x,z})^2 - \varepsilon_0(\varepsilon_{\parallel} n_x^2 + \varepsilon_{\perp} n_y^2) E_0^2] dz \quad (\text{twist geometry}), \quad (12a)$$

$$\mathcal{F}[\mathbf{n}] = \frac{1}{2} \int_0^d \left[K_1 n_{z,z}^2 + K_3 n_{x,z}^2 - \varepsilon_0 \frac{\varepsilon_{\perp} \varepsilon_{\parallel}}{\varepsilon_{\perp} n_x^2 + \varepsilon_{\parallel} n_z^2} E_0^2 \right] dz \quad (\text{bend geometry}). \quad (12b)$$

Thus, modeling the cases with in-plane electric fields in terms of the “outer solutions” ($\mathbf{n} = \mathbf{n}(z)$, $\mathbf{E} = \mathbf{E}(z)$) gives rise to reduced models $\mathcal{F} = \mathcal{F}[\mathbf{n}]$ that are *local*, in contrast to the non-local reduced model that one obtains for the electric-field splay-Fréedericksz transition. The reality of the matter is that the electric field at a point in Ω depends on the director field everywhere; however, in this geometry and asymptotic regime, the non-local contribution only serves as a small correction associated with the boundary-layer functions. The modeling of the electric field here is essentially equivalent to that done in [6]. If one wishes to model the electric-field twist and bend transitions in a way that is as close as possible to the way that the corresponding magnetic-field transitions are modeled, then one is led to make the assumptions made here (i.e., $\mathbf{n} = \mathbf{n}(z)$, $\mathbf{E} = \mathbf{E}(z)$).

4.3. Discussion

The basic assumption that the width of the cell is much smaller than the lateral dimensions is taken as a justification for assuming that equilibrium fields satisfy $\mathbf{n} = \mathbf{n}(z)$ and $\mathbf{E} = \mathbf{E}(z)$ (to a good degree of approximation). This underlies the modeling for all three electric-field Fréedericksz transitions, though it leads to different consequences in each case. In the splay geometry (the only case with a cross-plane electric field), the assumed functional dependence of \mathbf{n} and \mathbf{E} only on z enables one to derive the explicit formula for the electric field in terms of the director field given in (9). This expression is non-local, because it depends on $\int_0^d (\varepsilon_\perp n_x^2 + \varepsilon_\parallel n_z^2)^{-1} dz$, but it leads to the reduced free-energy functional (10), which is amenable to analysis.

For the geometries with in-plane electric fields (twist and bend), the same assumptions enable one to deduce explicit formulas for the electric field in terms of the director field that are local— $\mathbf{E}(z)$ depends only on the value of \mathbf{n} at the point z . In the twist case, the electric field is in fact *uniform* throughout the strip between the electrodes (which are viewed as being infinitely tall):

$$\mathbf{E} = E_0 \mathbf{e}_x, \quad -\infty < z < \infty.$$

While in the bend case, the electric field is uniform *outside* the cell, but inhomogeneity of the director field induces nonuniformity of the electric field *inside* the cell:

$$\mathbf{E} = E_0 \mathbf{e}_x + E_z(z) \mathbf{e}_z, \quad E_z = -\varepsilon_a E_0 \frac{n_x n_z}{\varepsilon_\perp n_x^2 + \varepsilon_\parallel n_z^2}, \quad 0 < z < d. \quad (13)$$

In all three cases, the formulas for the electric fields in terms of the director fields enable one to write the free energies as reduced functionals of \mathbf{n} only: (10), (12a), and (12b).

It is not difficult to see why these three cases differ. In the splay geometry, the electrodes are on the top and bottom, and the electric field is confined to the cell. The value of D_z is constant across the cell but *nonzero*, by virtue of the surface charge densities on the electrodes—with a charge density of σ_f on $z = d$ and $-\sigma_f$ on $z = 0$, we have $D_z = -\sigma_f$. To express this constant in terms of \mathbf{n} requires an integration $\int_0^d dz$ and results in the non-local expression in (9).

The twist and bend geometries both involve in-plane electric fields, and in both cases, the electric fields extend beyond the cell containing the liquid crystal to the whole region between the vertical electrodes, $-\infty < z < \infty$. For both cases, D_z is constant throughout this whole region, and this constant is in fact *zero*, by virtue of the far-field conditions ($\mathbf{E} \rightarrow E_0 \mathbf{e}_x$, as $z \rightarrow \pm\infty$). The relation $D_z = 0$ can be solved for E_z in terms of \mathbf{n} , resulting in the local expressions in (11a) and (11b). In both the twist geometry and the bend geometry, the equilibrium electric field is always uniform *outside* the cell, as well as *inside* the cell in the *ground state*: $\mathbf{E} = E_0 \mathbf{e}_x$. The equilibrium electric field maintains this same uniform structure in the cell for any *twist* deformation, while *bend* distortions of the director cause the electric field in the cell to develop inhomogeneity in the form (13). The reason why $E_z = 0$ in the cell for twist distortions but $E_z \neq 0$ for bend distortions can be understood in terms of the different nature of the *dielectric polarization* in the two cases.

There are two sources of contributions to the local electric field in the systems under consideration here: free charges on the surface of the electrodes and induced polarization in the dielectric medium. The electrodes are essentially accounted for in the horizontal component $E_0 \mathbf{e}_x$, the uniform electric field that one would have if the medium were homogeneous. The electric field associated with a polarization field \mathbf{P} in a volume Ω is the same as the field that would be created by an effective volume charge density ρ_P in Ω and surface charge density σ_P on the boundary $\partial\Omega$ given by

$$\rho_P = -\operatorname{div} \mathbf{P}, \quad \sigma_P = \mathbf{P} \cdot \boldsymbol{\nu},$$

where $\boldsymbol{\nu}$ is the outward unit normal on $\partial\Omega$. Under our modeling assumptions (transversely

isotropic material, linear dielectric regime), the induced polarization in the liquid-crystal layer is given by

$$\mathbf{P} = \chi_{\perp}^e \mathbf{E} + \Delta\chi^e (\mathbf{E} \cdot \mathbf{n}) \mathbf{n}, \quad \Delta\chi^e := \chi_{\parallel}^e - \chi_{\perp}^e, \quad (14)$$

where χ_{\parallel}^e and χ_{\perp}^e are the electric susceptibilities parallel to \mathbf{n} and perpendicular to \mathbf{n} . These are related to the electric permittivities through $\mathbf{D} = \varepsilon_0 \mathbf{E} + \mathbf{P}$ and (2):

$$\varepsilon_0 \varepsilon_{\perp} = \varepsilon_0 + \chi_{\perp}^e, \quad \varepsilon_0 \varepsilon_{\parallel} = \varepsilon_0 + \chi_{\parallel}^e, \quad \varepsilon_0 \varepsilon_a = \Delta\chi^e. \quad (15)$$

In the asymptotic regime of the outer solutions, $\mathbf{P} = \mathbf{P}(z)$, and all interfaces are horizontal ($\boldsymbol{\nu} = \pm \mathbf{e}_z$). It follows that

$$\rho_P = -P_{z,z}, \quad \sigma_P = \pm P_z.$$

The z component of \mathbf{P} is identically *zero* throughout the region between the electrodes *exterior* to the cell. Thus, in order for a polarization field \mathbf{P} in the liquid-crystal cell (in our asymptotic regime) to produce an electric field, it must be such that P_z has a non-vanishing z derivative in $0 < z < d$ or $P_z \neq 0$ on $z = 0+$ or $z = d-$.

If we contrast twist distortions with bend distortions in our geometry ($\mathbf{n} = n_x(z)\mathbf{e}_x + n_y(z)\mathbf{e}_y$ versus $\mathbf{n} = n_x(z)\mathbf{e}_x + n_z(z)\mathbf{e}_z$), assuming for the moment a uniform electric field $\mathbf{E} = E_0\mathbf{e}_x$, we obtain from (14)

$$P_z^{\text{twist}} = 0, \quad P_z^{\text{bend}} = \Delta\chi^e E_0 n_x n_z, \quad 0 < z < d.$$

Thus for twist distortions, $\rho_P = 0$ and $\sigma_P = 0$. Twist distortions give rise to changes in the x and y components of \mathbf{P} , but these are *uniform* in the x - y plane under our assumptions and do not contribute to $\text{div } \mathbf{P}$ ($P_{x,x} = P_{y,y} = 0$). Even though the twist-distorted director field has a nonzero z derivative, P_z is constant (zero) and does not. Thus a uniform electric field $\mathbf{E} = E_0\mathbf{e}_x$ is in electrostatic equilibrium with any twist configuration.

For bend distortions, $n_x = 0$ on $z = 0$ and $z = d$; so $\sigma_P = 0$, as with twist distortions. However,

$$P_{z,z}^{\text{bend}} = \Delta\chi^e E_0 \frac{\partial}{\partial z} (n_x n_z) \neq 0,$$

by virtue of the variation of \mathbf{n} in the z direction. Thus $\rho_P \neq 0$, and there is an associated *effective charge density*, which would give rise to additional contributions to \mathbf{E} . A uniform electric field $\mathbf{E} = E_0\mathbf{e}_x$ cannot be in equilibrium in a medium with such structure, which is why $E_z \neq 0$ is needed in (13) for bend distortions. The proper, full expression for P_z in the bend case is given by

$$P_z^{\text{bend}} = (\chi_{\perp}^e n_x^2 + \chi_{\parallel}^e n_z^2) E_z + \Delta\chi^e n_x n_z E_0,$$

but we still have $\sigma_P = 0$, since $P_z^{\text{bend}} = 0$ at $z = 0$ and $z = d$, due to the vanishing of both n_x and E_z on the boundaries of the cell:

$$E_z = -\varepsilon_a E_0 \frac{n_x n_z}{\varepsilon_{\perp} n_x^2 + \varepsilon_{\parallel} n_z^2}, \quad n_x(0) = n_x(d) = 0.$$

The fact that $E_z \neq 0$ in the case of bend distortions is entirely due to the effective space charge from the induced polarization, which is absent in the case of twist distortions. Whether E_z is positive or negative, it leads to an increased magnitude of the local electric field, $E^2 = E_0^2 + E_z^2 > E_0^2$, and it emerges as soon as \mathbf{n} is perturbed from \mathbf{n}_0 (producing $n_x \neq 0$ above). It is

also the case that the additional electric-field component is in the z direction, which is *aligning* and weakens the dielectric torque that is trying to rotate the director towards the horizontal.

The situation for electric-field Fréedericksz transitions with $\varepsilon_a > 0$ then is the following. The splay transition is well analyzed in [9] and [10], and a good textbook account is given in [5, Sec. 3.5]. The instability threshold follows the magnetic-field analogy, and the transition is second order for all relevant parameter values. None of this is in question here. The twist transition is modeled by the free energy (12a), and as discussed above, the equilibrium electric field remains *uniform* for any twist distortions. Thus the analysis of the electric-field twist-Fréedericksz transition is completely aligned with that of the associated magnetic-field transition. One concludes that the local instability threshold is

$$E_c = \frac{\pi}{d} \sqrt{\frac{K_2}{\varepsilon_0 \varepsilon_a}}$$

and that the transition is second order for any $K_2 > 0$ and $\varepsilon_{\parallel} > \varepsilon_{\perp} > 0$. The magnetic-field analogy again holds. The only case that requires further analysis is the electric-field bend-Fréedericksz transition, which we take up next.

5. Analysis of the electric-field bend-Fréedericksz transition

The electric-field bend-Fréedericksz transition is modeled in terms of the free energy (12b), which can be analyzed in various ways. Here we utilize a *perturbation expansion* to identify and study the bifurcation at the point at which the uniform ground-state solution of the Euler-Lagrange equations ceases to be locally stable. This type of analytical approach has been widely used in the area of liquid crystals by Schiller (see the review article [18]) and others [19, 20].

We represent the director in terms of its tilt angle as

$$\mathbf{n} = \sin \theta \mathbf{e}_x + \cos \theta \mathbf{e}_z, \quad \theta = \theta(z),$$

for which the ground state corresponds to $\theta = 0$. In terms of this representation, the free-energy functional (12b) takes the form

$$\mathcal{F}[\theta] = \frac{1}{2} \int_0^d \left[(K_1 \sin^2 \theta + K_3 \cos^2 \theta) \theta_{,z}^2 - \varepsilon_0 \frac{\varepsilon_{\perp} \varepsilon_{\parallel}}{\varepsilon_{\perp} \sin^2 \theta + \varepsilon_{\parallel} \cos^2 \theta} E_0^2 \right] dz.$$

We employ the following non-dimensionalization:

$$\begin{aligned} \bar{\mathcal{F}}[\bar{\theta}] &= \frac{1}{2} \int_0^{\pi} \left[(1 + \alpha_K \sin^2 \bar{\theta}) \bar{\theta}_{,\bar{z}}^2 - \gamma \frac{1}{1 - \alpha_{\varepsilon} \sin^2 \bar{\theta}} \right] d\bar{z} \\ \bar{\mathcal{F}} &= \frac{\mathcal{F}}{K_3 \pi / d}, \quad \bar{z} = \frac{\pi z}{d}, \quad \bar{\theta}(\bar{z}) = \theta(z) \\ \alpha_K &:= \frac{K_1 - K_3}{K_3}, \quad \alpha_{\varepsilon} := \frac{\varepsilon_{\parallel} - \varepsilon_{\perp}}{\varepsilon_{\parallel}}, \quad \gamma := \frac{\varepsilon_0 \varepsilon_{\perp} E_0^2}{K_3 \pi^2 / d^2}. \end{aligned} \tag{16}$$

The dimensionless parameters α_K and α_{ε} represent the relative anisotropies of the elastic constants and dielectric constants, while the coupling constant γ reflects the relative strength of the electric field compared to distortional elasticity.

Equilibrium states are solutions of the associated Euler-Lagrange equation, which (after dropping bars) is given by

$$\frac{d}{dz} \left[(1 + \alpha_K \sin^2 \theta) \frac{d\theta}{dz} \right] + \sin \theta \cos \theta \left[\frac{\gamma \alpha_{\varepsilon}}{(1 - \alpha_{\varepsilon} \sin^2 \theta)^2} - \alpha_K \left(\frac{d\theta}{dz} \right)^2 \right] = 0, \quad \theta(0) = \theta(\pi) = 0. \tag{17}$$

The ground state $\theta = 0$ is a solution for any values of α_K , α_ε , and γ . We view γ as the *control parameter* and wish to determine for what value of γ (given α_K and α_ε) the ground state becomes locally unstable and the nature of the branch of nonuniform equilibrium solutions that bifurcates from the ground-state branch at that point. We parameterize the bifurcating branch in terms of a parameter η and assume the validity of the expansions

$$\begin{aligned}\theta(z; \eta) &= \eta \theta_1(z) + \eta^3 \theta_3(z) + \dots \\ \gamma(\eta) &= \gamma_0 + \gamma_2 \eta^2 + \gamma_4 \eta^4 + \dots\end{aligned}\tag{18}$$

for small η (the ground state corresponding to $\eta = 0$). The assumed form (18) is based upon problem symmetry: if the scalar field θ is a solution of (17), then so is $-\theta$. There is no intrinsic scale for the parameter η , and we find it convenient to normalize it via

$$w_1 \left(\frac{d\gamma}{d\eta} \right)^2 + w_2 \int_0^\pi \left(\frac{d\theta}{d\eta} \right)^2 dz = \text{const},\tag{19}$$

using the values $w_1 = 6\pi\alpha_\varepsilon^2$, $w_2 = 2$, and $\text{const} = \pi$ for convenience in what follows. The parameter η can be viewed as a type of “pseudo arc-length” in γ - θ space. At the first three orders, the normalization condition gives rise to constraints

$$\begin{aligned}O(1): \quad & w_2 \int_0^\pi \theta_1^2 dz = \text{const} \\ O(\eta): \quad & 0 = 0 \\ O(\eta^2): \quad & 2w_1\gamma_2^2 + 3w_2 \int_0^\pi \theta_1\theta_3 dz = 0.\end{aligned}$$

Substituting the expansions for θ and γ into the Euler-Lagrange equation and boundary conditions, we obtain at order $O(\eta)$

$$\frac{d^2\theta_1}{dz^2} + \gamma_0\alpha_\varepsilon\theta_1 = 0, \quad \theta_1(0) = \theta_1(\pi) = 0,$$

for which the first nontrivial bifurcating solution is given by

$$\gamma_0\alpha_\varepsilon = 1, \quad \theta_1 = c_{1,1} \sin z,$$

with the constant $c_{1,1}$ to be determined. Using this expression for θ_1 in the normalization condition at order $O(1)$ gives

$$w_2 c_{1,1}^2 \int_0^\pi \sin^2 z dz = w_2 c_{1,1}^2 \frac{\pi}{2} = \text{const}.$$

With our choices $w_2 = 2$ and $\text{const} = \pi$, the above yields $c_{1,1} = \pm 1$. Choosing $c_{1,1} = 1$ determines $\theta_1 = \sin z$.

The problem for θ_3 arises at order $O(\eta^3)$:

$$\frac{d^2\theta_3}{dz^2} + \theta_3 + a_{3,1} \sin z + a_{3,3} \sin 3z = 0, \quad \theta_3(0) = \theta_3(\pi) = 0,$$

with

$$a_{3,1} = \frac{1}{2}[(3 + 2\gamma_2)\alpha_\varepsilon - \alpha_K - 1], \quad a_{3,3} = \frac{1}{6}(3\alpha_K - 3\alpha_\varepsilon + 1).$$

Solvability requires that $a_{3,1} = 0$ (see [21, Ch. 15]), giving

$$\gamma_2 \alpha_\varepsilon = \frac{1}{2}(\alpha_K - 3\alpha_\varepsilon + 1).$$

The solution θ_3 then becomes

$$\theta_3 = c_{3,1} \sin z + c_{3,3} \sin 3z, \quad c_{3,3} = \frac{1}{48}(3\alpha_K - 3\alpha_\varepsilon + 1), \quad (20)$$

with $c_{3,1}$ to be determined. Substituting the expressions for γ_2 , θ_1 , and θ_3 into the normalization condition at order $O(\eta^2)$ produces

$$w_1 \left(\frac{\alpha_K - 3\alpha_\varepsilon + 1}{\alpha_\varepsilon} \right)^2 + 3\pi w_2 c_{3,1} = 0,$$

which gives

$$c_{3,1} = -(\alpha_K - 3\alpha_\varepsilon + 1)^2 \quad (21)$$

using our chosen weights $w_1 = 6\pi\alpha_\varepsilon^2$ and $w_2 = 2$.

At this stage, we have all the information that we require. In terms of our dimensionless variables, we have

$$\begin{aligned} \theta &= \eta \sin z + \eta^3 (c_{3,1} \sin z + c_{3,3} \sin 3z) + \dots \\ \alpha_\varepsilon \gamma &= 1 + \frac{1}{2}(\alpha_K - 3\alpha_\varepsilon + 1)\eta^2 + \dots, \end{aligned}$$

with $c_{3,1}$ and $c_{3,3}$ as given in (21) and (20). Our choice of weights in (19) has led to a normalization in which the parameter η corresponds to the *amplitude* of the leading instability mode, the longest-wavelength mode $\sin \bar{z}$. In terms of the original variables, the expansions read

$$\begin{aligned} \theta &= \eta \sin \frac{\pi z}{d} + \eta^3 \left\{ -\left(\frac{K_1}{K_3} - 3 \frac{\varepsilon_a}{\varepsilon_\parallel} \right)^2 \sin \frac{\pi z}{d} \right. \\ &\quad \left. + \frac{1}{48} \left[3 \left(\frac{K_1}{K_3} - \frac{\varepsilon_a}{\varepsilon_\parallel} \right) - 2 \right] \sin \frac{3\pi z}{d} \right\} + \dots \\ E_0^2 &= \frac{\varepsilon_\parallel}{\varepsilon_\perp} \frac{\pi^2}{d^2} \frac{K_3}{\varepsilon_0 \varepsilon_a} \left[1 + \frac{1}{2} \left(\frac{K_1}{K_3} - 3 \frac{\varepsilon_a}{\varepsilon_\parallel} \right) \eta^2 + \dots \right]. \end{aligned}$$

We see that the critical threshold here is *elevated* from that predicted by the magnetic-field analogy:

$$E_c = \frac{\pi}{d} \sqrt{\frac{\varepsilon_\parallel}{\varepsilon_\perp}} \sqrt{\frac{K_3}{\varepsilon_0 \varepsilon_a}}, \quad \text{with } \frac{\varepsilon_\parallel}{\varepsilon_\perp} > 1 \quad \text{vs} \quad E_c = \frac{\pi}{d} \sqrt{\frac{K_3}{\varepsilon_0 \varepsilon_a}} \leftrightarrow H_c = \frac{\pi}{d} \sqrt{\frac{K_3}{\chi_a}}.$$

The sign of the coefficient in front of η^2 in the expansion for E_0^2 above indicates whether the bifurcation is *super-critical* (positive coefficient) or *sub-critical* (negative coefficient). The former case ($K_1/K_3 - 3\varepsilon_a/\varepsilon_\parallel > 0$) is consistent with a *second-order* transition, while the latter would be associated with a transition of *first order*.

The formulas above for the critical threshold and the crossover from first order to second order agree with predictions in [6], where they were deduced in a different way. The question of when a Fréedericksz transition can be first order has been well studied elsewhere—see [17] and references contained therein. We note that the elevation of the threshold here is *not small*:

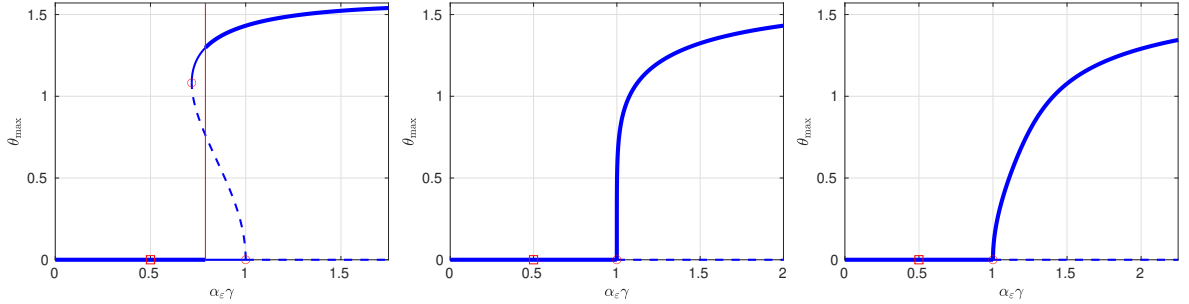


Figure 3. Upper halves of bifurcation diagrams for electric-field bend-Fréedericksz transitions in terms of reduced units as defined in (16). Maximum tilt angle θ_{\max} versus reduced electric field strength $\alpha_\varepsilon\gamma$. Dashed line (locally unstable), solid line (locally stable, metastable), heavy solid line (globally stable, minimum free energy). For all three figures, the relative dielectric anisotropy is fixed at $\alpha_\varepsilon = 0.5$. The relative anisotropy of the elastic constants varies as follows: $\alpha_K = -0.5$ (left, first-order transition), 0.5 (center, crossover), 1.5 (right, second-order transition). The boxes on the horizontal axes are at the location of the instability threshold predicted by the magnetic-field analogy (treating the electric field as uniform), given by $\alpha_\varepsilon\gamma = 1 - \alpha_\varepsilon = 0.5$ in these units.

using data from [5, Table D.3] for the liquid-crystal material 5CB near 26°C, we have

$$\varepsilon_{\parallel} = 18.5, \quad \varepsilon_{\perp} = 7 \quad \Rightarrow \quad \sqrt{\frac{\varepsilon_{\parallel}}{\varepsilon_{\perp}}} \doteq 1.63,$$

a 63% increase. For the same material and temperature (with data from the same source), we have $K_1 = 6.2 \times 10^{-12}$ J/m and $K_3 = 8.2 \times 10^{-12}$ J/m. With these material parameters, the quantity $K_1/K_3 - 3\varepsilon_a/\varepsilon_{\parallel} = -1.1 < 0$; so the transition should be *first order*, as was found in experiments reported in [11, 12].

In Figure 3, the upper halves of bifurcation diagrams are plotted for three sets of dimensionless parameters based upon numerical modeling of (17) using a numerical bifurcation package, as described in [13, Secs. 6.2 and 6.3]. The parameter values were chosen to illustrate the crossover from a first-order transition to a second-order transition, which occurs at $\alpha_K = 0.5$ when $\alpha_\varepsilon = 0.5$ (as in Figure 3). The phenomena of an elevated local instability threshold and a first-order transition can be seen as related: the elevation of the threshold necessitates a subcritical bifurcation in order for the branch to reach distorted equilibrium configurations of the director field that are locally stable for electric-field strengths of lesser amounts (for certain combinations of material constants).

The natural question at this point is why the local-instability threshold is elevated for the electric-field bend transition but not for the splay or twist transitions. A partial answer has already been provided by the observation that the electric field remains *uniform* for *twist* distortions but develops *inhomogeneity* with *bend* distortions. This does not explain, however, why this should lead to an elevation of the instability threshold—in the splay geometry, inhomogeneity of the electric field develops as well, but that does not lead to an elevation of the threshold. An answer is provided by a careful development of a criterion for local stability of a coupled director field and electric field, generalizing (6) and (7). This was done in a general setting in [7] and is discussed next.

6. Electric-field-induced instabilities

Whether the coupling between the electric field and the director field will affect the threshold of local instability depends on *dielectric polarization*, in particular on how the induced polarization changes at a bifurcation from a branch of ground-state director configurations. We illustrate this by presenting a necessary condition for local stability and showing how it correctly predicts the behaviors that we have observed with the three basic electric-field Fréedericksz transitions. Additional examples are given that evidence the broader applicability of the development, including systems involving twisted nematics, planar cholesterics, smectic-A phases, and nematic

films that exhibit periodic instabilities.

6.1. A necessary condition for local stability

As modeled by the free-energy functional \mathcal{F}_E in (4), a locally stable director field \mathbf{n} will be a local minimizer of $\mathcal{F}_E[\mathbf{n}, \varphi]$ subject to the constraints

$$|\mathbf{n}| = 1 \quad \text{and} \quad \text{div}[\boldsymbol{\varepsilon}(\mathbf{n})\nabla\varphi] = 0, \quad \text{on } \Omega,$$

plus appropriate boundary conditions on both \mathbf{n} and φ . As such, a sufficiently smooth \mathbf{n} must necessarily satisfy the Euler-Lagrange equations

$$-\text{div}\left(\frac{\partial W_e}{\partial \nabla \mathbf{n}}\right) + \frac{\partial W_e}{\partial \mathbf{n}} = \lambda \mathbf{n} + \varepsilon_0 \varepsilon_a (\nabla \varphi \cdot \mathbf{n}) \nabla \varphi, \quad \text{on } \Omega. \quad (22)$$

In order to determine if an equilibrium pair $(\mathbf{n}_0, \varphi_0)$ is locally minimizing, we require an expression for $\mathcal{F}_E[\mathbf{n}, \varphi]$ for admissible pairs (\mathbf{n}, φ) close to $(\mathbf{n}_0, \varphi_0)$, generalizing (6).

A perturbation of the director field $\mathbf{n}_0 \mapsto \mathbf{n}_0 + \epsilon \mathbf{u}$ will satisfy all the constraints on \mathbf{n} to first order in ϵ if \mathbf{u} is *transverse* to \mathbf{n}_0 ($\mathbf{n}_0 \cdot \mathbf{u} = 0$ on Ω) and satisfies *homogeneous* boundary conditions on $\partial\Omega$. We need to know under what conditions a perturbation $(\mathbf{n}_0, \varphi_0) \mapsto (\mathbf{n}_0 + \epsilon \mathbf{u}, \varphi_0 + \epsilon \psi)$ will satisfy to first order the constraint on φ as well (namely $\text{div}[\boldsymbol{\varepsilon}(\mathbf{n})\nabla\varphi] = 0$). To deduce this, we use (2) to expand

$$\boldsymbol{\varepsilon}(\mathbf{n}_0 + \epsilon \mathbf{u})\nabla(\varphi_0 + \epsilon \psi) = \boldsymbol{\varepsilon}(\mathbf{n}_0)\nabla\varphi_0 + \epsilon [\Delta\chi^e(\mathbf{n}_0 \otimes \mathbf{u} + \mathbf{u} \otimes \mathbf{n}_0)\nabla\varphi_0 + \boldsymbol{\varepsilon}(\mathbf{n}_0)\nabla\psi] + O(\epsilon^2).$$

Here we have also used $\varepsilon_0 \varepsilon_a = \Delta\chi^e$ from (15) to express the above in terms of electric susceptibilities. Since $\text{div}[\boldsymbol{\varepsilon}(\mathbf{n}_0)\nabla\varphi_0] = 0$ by assumption, in order for the constraint $\text{div}[\boldsymbol{\varepsilon}(\mathbf{n})\nabla\varphi] = 0$ to be preserved at first order, ψ must satisfy

$$\text{div}[\boldsymbol{\varepsilon}(\mathbf{n}_0)\nabla\psi] = \text{div} \mathbf{p}_0, \quad \text{on } \Omega, \quad (23a)$$

where

$$\mathbf{p}_0 := \Delta\chi^e(\mathbf{n}_0 \otimes \mathbf{u} + \mathbf{u} \otimes \mathbf{n}_0)\mathbf{E}_0, \quad \mathbf{E}_0 = -\nabla\varphi_0. \quad (23b)$$

As is the case with the director field and its perturbations, the field ψ must be such that $\varphi_0 + \epsilon\psi$ satisfies the boundary conditions that φ must satisfy. While more general conditions are considered in [7], here we assume, for simplicity, that the electric potential φ is fixed on the entire boundary $\partial\Omega$, which implies that all such perturbative fields ψ must *vanish* on $\partial\Omega$. Thus, given an equilibrium pair $(\mathbf{n}_0, \varphi_0)$ and director perturbation $\mathbf{n}_0 \mapsto \mathbf{n}_0 + \epsilon \mathbf{u}$, the associated perturbation of the electric potential $\varphi_0 \mapsto \varphi_0 + \epsilon\psi$ must satisfy an electrostatic potential problem consisting of (23a) plus homogeneous boundary conditions on $\partial\Omega$.

The vector field \mathbf{p}_0 represents the *first-order* change in induced polarization associated with the perturbation $\mathbf{n}_0 \mapsto \mathbf{n}_0 + \epsilon \mathbf{u}$, and $-\text{div} \mathbf{p}_0$ acts as an effective *volume charge density* driving ψ and the associated perturbation of the electric field $\mathbf{E}_0 \mapsto \mathbf{E}_0 - \epsilon \nabla\psi$. The only solution of $\text{div}[\boldsymbol{\varepsilon}(\mathbf{n}_0)\nabla\psi] = 0$ satisfying $\psi = 0$ on $\partial\Omega$ is the *zero solution*, and we conclude that

$$\psi = 0 \quad \text{on } \Omega \quad \text{if and only if} \quad \text{div} \mathbf{p}_0 = 0 \quad \text{on } \Omega.$$

Thus if $\text{div} \mathbf{p}_0 = 0$ on Ω , then the constraint $\text{div}[\boldsymbol{\varepsilon}(\mathbf{n})\nabla\varphi] = 0$ will be preserved to first order under the perturbation $\mathbf{n}_0 \mapsto \mathbf{n}_0 + \epsilon \mathbf{u}$ with an *unperturbed* electric field $\mathbf{E}_0 = -\nabla\varphi_0$. Changes in the director field cause changes in the electric field in general, but in the case $\text{div} \mathbf{p}_0 = 0$, these changes come in at *higher order*. Making use of the information gleaned thus far, the following is established in [7].

Let $(\mathbf{n}_0, \varphi_0)$ be an equilibrium pair associated with \mathcal{F}_E in (4) as above, and let $(\mathbf{n}_\epsilon, \varphi_\epsilon)$ be an admissible pair perturbed from $(\mathbf{n}_0, \varphi_0)$ constructed in the form

$$\mathbf{n}_\epsilon = \frac{\mathbf{n}_0 + \epsilon \mathbf{v}}{|\mathbf{n}_0 + \epsilon \mathbf{v}|}, \quad \text{div}[\boldsymbol{\varepsilon}(\mathbf{n}_\epsilon) \nabla \varphi_\epsilon] = 0,$$

where $\mathbf{v} = \mathbf{0}$ on $\partial\Omega$ and the potential φ_ϵ satisfies the boundary conditions that φ must satisfy. The free energy $\mathcal{F}_E[\mathbf{n}_\epsilon, \varphi_\epsilon]$ admits the following expansion for small ϵ :

$$\mathcal{F}_E[\mathbf{n}_\epsilon, \varphi_\epsilon] = \mathcal{F}_E[\mathbf{n}_0, \varphi_0] + \frac{1}{2} \epsilon^2 \left[\delta_{\mathbf{nn}}^2 \mathcal{F}_E[\mathbf{n}_0, \varphi_0](\mathbf{u}) + \int_{\Omega} \boldsymbol{\varepsilon}(\mathbf{n}_0) \nabla \psi \cdot \nabla \psi \, dV - \int_{\Omega} \lambda_0 |\mathbf{u}|^2 \, dV \right] + o(\epsilon^2),$$

where $\mathbf{u} = \mathbf{P}(\mathbf{n}_0) \mathbf{v}$ as in (5) and ψ solves the problem (23a) with $\psi = 0$ on $\partial\Omega$. Here λ_0 is the Lagrange multiplier field associated with the solution \mathbf{n}_0 of (22), and $\delta_{\mathbf{nn}}^2 \mathcal{F}_E$ denotes the second variation of \mathcal{F}_E with respect to \mathbf{n} :

$$\delta_{\mathbf{nn}}^2 \mathcal{F}_E[\mathbf{n}, \varphi](\mathbf{v}) = \int_{\Omega} \left(\frac{\partial^2 W}{\partial n_i \partial n_k} v_i v_k + 2 \frac{\partial^2 W}{\partial n_i \partial n_{k,l}} v_i v_{k,l} + \frac{\partial^2 W}{\partial n_{i,j} \partial n_{k,l}} v_{i,j} v_{k,l} \right) dV,$$

$$W = W_e - \frac{1}{2} \boldsymbol{\varepsilon}(\mathbf{n}) \nabla \varphi \cdot \nabla \varphi.$$

We conclude that in order for an equilibrium director field \mathbf{n}_0 with associated Lagrange multiplier field λ_0 and coupled electric potential field φ_0 to be *locally stable*, it must necessarily satisfy

$$\delta_{\mathbf{nn}}^2 \mathcal{F}_E[\mathbf{n}_0, \varphi_0](\mathbf{u}) + \int_{\Omega} \boldsymbol{\varepsilon}(\mathbf{n}_0) \nabla \psi \cdot \nabla \psi \, dV - \int_{\Omega} \lambda_0 |\mathbf{u}|^2 \, dV \geq 0 \quad (24)$$

for all test fields \mathbf{u} that are transverse to \mathbf{n}_0 ($\mathbf{n}_0 \cdot \mathbf{u} = 0$ on Ω) and satisfy $\mathbf{u} = \mathbf{0}$ on $\partial\Omega$, with the scalar field ψ (which depends on \mathbf{u}) the solution of (23a) subject to $\psi = 0$ on $\partial\Omega$.

The necessary condition above generalizes (7). The first and third terms in (24) are already present in (7); while the second term is new. The integral involving λ_0 is again associated with the pointwise constraint $|\mathbf{n}| = 1$. The second term is associated with the constraint on the electric potential ($\text{div}[\boldsymbol{\varepsilon}(\mathbf{n}) \nabla \varphi] = 0$) and compensates for the fact that the perturbation ψ preserves this only to first order. The perturbation of the electric potential, ψ , is slaved to the perturbation of the director field, \mathbf{u} , just as the electric potential φ is slaved to the director field \mathbf{n} . The dielectric tensor $\boldsymbol{\varepsilon}(\mathbf{n}_0)$ is *positive definite*; so the middle term in (24) is *strictly positive* unless $\nabla \psi$ is *identically zero* on Ω . The presence of a positive second term in (24) increases the energy barrier that must be overcome to destabilize the ground state, and it is this term that causes the increase in the local-instability threshold. That this middle term is *nonnegative* emerges in a natural way in the calculus of deriving (24) (see [7]); the nonnegativity can be viewed as a consequence of the minimax nature of the problem. A perturbation of a ground state director field will cause a change in the induced polarization in general; the discriminating factor is whether this leads to a *first-order* or *higher-order* effect.

In an electric-field transition, then, there are *two* stabilizing influences: distortional elasticity (which penalizes nonuniformity of the director field) and electrostatic energy (which penalizes spontaneous additions to the electric field). The former is present in magnetic-field transitions; the latter is not. The necessary condition for local stability (24) provides us with two useful pieces of information. First, it shows us that the coupling between the electric field and the director field can influence an instability threshold only if there exists a director perturbation \mathbf{u} for which $\text{div} \mathbf{p}_0$ is *not* identically zero on Ω , since this is the only way to obtain a ψ such that $\nabla \psi$ is not identically zero on Ω , and second, it shows us that the effect can only be to *elevate* an instability threshold, *never* to *lower* it (since the middle term in (24) can only be *positive* or

zero). The criterion involving $\text{div } \mathbf{p}_0$ provides a simple test for when the coupling between the director field and the electric field can cause an elevated threshold, which we now demonstrate.

6.2. Application to classical electric-field Fréedericksz transitions

Our test for electric-field-induced transitions involves the first-order change in induced polarization \mathbf{p}_0 in (23b) and is the following.

If $\text{div } \mathbf{p}_0 = 0$ on Ω for *all* admissible director variations \mathbf{u} , then the instability threshold will *not* be elevated and will conform to the magnetic-field analogy. If, however, there exists an admissible variation \mathbf{u} such that $\text{div } \mathbf{p}_0$ is *not* identically zero on Ω , then the instability threshold *will* be elevated.

We show how this test can be applied to the electric-field splay, twist, and bend Fréedericksz transitions (with $\varepsilon_a > 0$).

The splay geometry is illustrated in Figure 1 left, with the director field confined to the x - z tilt plane ($\mathbf{n} = n_x(z)\mathbf{e}_x + n_z(z)\mathbf{e}_z$). The ground-state director field \mathbf{n}_0 , ground-state electric field \mathbf{E}_0 , and admissible director variations \mathbf{u} are given by

$$\mathbf{n}_0 = \mathbf{e}_x, \quad \mathbf{E}_0 = E_0\mathbf{e}_z, \quad \mathbf{u} = w(z)\mathbf{e}_z,$$

where w is a sufficiently smooth function satisfying $w(0) = w(d) = 0$. In terms of these, \mathbf{p}_0 takes the form

$$\mathbf{p}_0 = \Delta\chi^e(\mathbf{n}_0 \otimes \mathbf{u} + \mathbf{u} \otimes \mathbf{n}_0)\mathbf{E}_0 = \Delta\chi^e[(\mathbf{u} \cdot \mathbf{E}_0)\mathbf{n}_0 + (\mathbf{n}_0 \cdot \mathbf{E}_0)\mathbf{u}] = \Delta\chi^e E_0 w(z)\mathbf{e}_x,$$

and it follows that

$$\text{div } \mathbf{p}_0 = \Delta\chi^e E_0 \frac{\partial}{\partial x} w(z) = 0$$

for all such perturbations \mathbf{u} . We conclude that the instability threshold should *not* be elevated, which is consistent with the analyses in [9], [10], and [5, Sec. 3.5]. The twist geometry (Figure 1 center) yields a similar result:

$$\begin{aligned} \mathbf{n}_0 &= \mathbf{e}_y, \quad \mathbf{E}_0 = E_0\mathbf{e}_x, \quad \mathbf{u} = v(z)\mathbf{e}_x \\ \mathbf{p}_0 &= \Delta\chi^e E_0 v(z)\mathbf{e}_y \Rightarrow \text{div } \mathbf{p}_0 = \Delta\chi^e E_0 \frac{\partial}{\partial y} v(z) = 0. \end{aligned}$$

Again, no elevation of the instability threshold is expected, consistent with our analysis in Section 4.

Only in the case of the bend geometry (Figure 1 right) do we encounter a departure from the script, for in that case,

$$\begin{aligned} \mathbf{n}_0 &= \mathbf{e}_z, \quad \mathbf{E}_0 = E_0\mathbf{e}_x, \quad \mathbf{u} = u(z)\mathbf{e}_x \\ \mathbf{p}_0 &= \Delta\chi^e E_0 u(z)\mathbf{e}_z \Rightarrow \text{div } \mathbf{p}_0 = \Delta\chi^e E_0 \frac{\partial}{\partial z} u(z) \neq 0. \end{aligned}$$

In this case, the first-order change in the induced polarization is *not* divergence free for all admissible \mathbf{u} , and there will be corresponding *positive* middle terms in (24), which will lead to an elevated instability threshold (as predicted in [6] and confirmed by our analysis in Section 5). It is possible to use (24) to deduce the formula for the elevated threshold,

$$E_c^2 = \frac{\varepsilon_{\parallel}}{\varepsilon_{\perp}} \frac{\pi^2}{d^2} \frac{K_3}{\varepsilon_0 \varepsilon_a}.$$

See [7, Sec. 4.2].

In both the splay geometry and the bend geometry, inhomogeneity of the electric field is brought about by the Fréedericksz transition. The difference between the two is that in the splay geometry, this is a *second-order* effect, while in the bend geometry, it is *first order*. This can be seen by a closer examination of the changes in polarization that are caused by the changes in the director field at the onset of the instability, which we now show.

In the splay geometry, at the instability onset (with the electric field treated as uniform), we have

$$\mathbf{E} = E_0 \mathbf{e}_z, \quad \mathbf{n} = \cos \theta \mathbf{e}_x + \sin \theta \mathbf{e}_z, \quad \theta = \theta(z),$$

where θ is *small* and satisfies $\theta(0) = \theta(d) = 0$, the ground state $\mathbf{n}_0 = \mathbf{e}_x$ corresponding to $\theta = 0$. From (14), the polarization is given by

$$\mathbf{P} = \chi_{\perp}^e E_0 \mathbf{e}_z + \Delta \chi^e E_0 \sin \theta (\cos \theta \mathbf{e}_x + \sin \theta \mathbf{e}_z),$$

so that $\mathbf{P}_0 = \chi_{\perp}^e E_0 \mathbf{e}_z$ in the ground state, and the change at onset (for small θ) is

$$\mathbf{P} - \mathbf{P}_0 = \Delta \chi^e E_0 [\theta(z) \mathbf{e}_x + \theta(z)^2 \mathbf{e}_z + O(\theta^3)].$$

Thus there is a first-order change in the \mathbf{e}_x component of $\mathbf{P} - \mathbf{P}_0$. All fields are assumed to be *uniform* in x and y , however; so this does not affect $\text{div } \mathbf{P}$. The change in the \mathbf{e}_z component is *second order* in θ , and as a consequence, *no change* in the electric field is needed to preserve $\text{div } \mathbf{D} = 0$ to first order—a second-order change in \mathbf{E} suffices to maintain $\text{div } \mathbf{D} = 0$ at second order.

In the bend geometry, on the other hand, we have

$$\mathbf{E} = E_0 \mathbf{e}_x, \quad \mathbf{n} = \sin \theta \mathbf{e}_x + \cos \theta \mathbf{e}_z,$$

giving

$$\mathbf{P} = \chi_{\perp}^e E_0 \mathbf{e}_x + \Delta \chi^e E_0 \sin \theta (\sin \theta \mathbf{e}_x + \cos \theta \mathbf{e}_z)$$

and

$$\mathbf{P} - \mathbf{P}_0 = \Delta \chi^e E_0 [\theta(z) \mathbf{e}_z + \theta(z)^2 \mathbf{e}_x + O(\theta^3)].$$

The change in the \mathbf{e}_z component is now *first order* in θ (the same as $\mathbf{p}_0 = \Delta \chi^e E_0 u(z) \mathbf{e}_z$ previously), and a first-order change in \mathbf{E} is required to maintain $\text{div } \mathbf{D} = 0$.

Closely related to the electric-field bend-Fréedericksz transition with $\varepsilon_a > 0$ above is the splay transition with $\varepsilon_a < 0$ (Figure 2 left), for which

$$\mathbf{E} = E_0 \mathbf{e}_x, \quad \mathbf{n} = \cos \theta \mathbf{e}_x + \sin \theta \mathbf{e}_z.$$

For this we have

$$\mathbf{P} = \chi_{\perp}^e E_0 \mathbf{e}_x + \Delta \chi^e E_0 \cos \theta (\cos \theta \mathbf{e}_x + \sin \theta \mathbf{e}_z),$$

which gives

$$\mathbf{P} - \mathbf{P}_0 = \Delta \chi^e E_0 [(\cos^2 \theta - 1) \mathbf{e}_x + \sin \theta \cos \theta \mathbf{e}_z] = \Delta \chi^e E_0 [-\theta(z)^2 \mathbf{e}_x + \theta(z) \mathbf{e}_z + O(\theta^3)],$$

and the first-order change in the \mathbf{e}_z component again necessitates a first-order correction in \mathbf{E} in order to maintain $\text{div } \mathbf{D} = 0$. The distinction rests entirely on the relative orientations of the

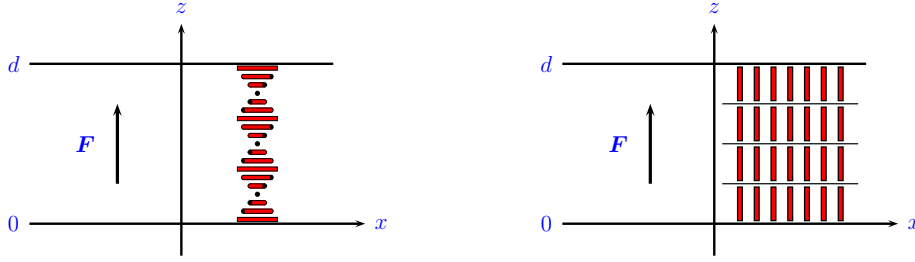


Figure 4. Other systems with instabilities induced by *magnetic* or *electric* fields ($\mathbf{F} = \mathbf{H}$ or $\mathbf{F} = \mathbf{E}$): *twisted nematic* or *cholesteric* (left, $\chi_a > 0$ or $\varepsilon_a > 0$), *smectic A* (right, $\chi_a < 0$ or $\varepsilon_a < 0$).

ground-state director field \mathbf{n}_0 , the ground-state electric field \mathbf{E}_0 , and the admissible variations of the director field \mathbf{u} (and the spatial dependencies of these).

6.3. Applications to generalized Fréedericksz transitions

In addition to the classical Fréedericksz transitions, there are other examples of field-induced instabilities in liquid-crystal systems, which are sometimes referred to as “generalized Fréedericksz transitions,” and the necessary condition for local stability (24) applies to them as well. It is also the case that the coupling between a director field and an electric field is essentially the same in any liquid-crystal phase; so while the criterion (24) and related ideas were developed in [7] in the context of a *nematic* liquid crystal, it is expected that they remain valid for *cholesteric* and *smectic* liquid crystals, for example. In this section, we consider some cases from these broader areas.

6.3.1. Twisted nematics and cholesterics

Planar twisted configurations of the form in Figure 4 left can be realized with nematic liquid crystals under the influence of boundary conditions or with cholesteric materials, for which such twisting states are natural even in the absence of any boundary influence. Ground states for director fields of the type pictured have the form

$$\mathbf{n}_0 = \cos q_0 z \mathbf{e}_x + \sin q_0 z \mathbf{e}_y.$$

It is known that for modest values of $q_0 d$, materials with positive anisotropy will, at a critical field strength, undergo a transition of Fréedericksz type to a distorted configuration that remains uniform in x and y but has a non-vanishing z component of the director. This basic, well-studied instability underlies the functioning of the “Twisted Nematic Cell” (TNC) and “Supertwisted Nematic” (STN) device, for which $q_0 d = \pi/2$ and $3\pi/2$ respectively [5, Sec. 3.7]. The necessary condition for local stability in (24) and associated test in Section 6.2 correctly indicate that there should be *no elevation* of the local instability threshold in such systems when using an electric field instead of magnetic field (with the magnetic parameters replaced by appropriate electric parameters in the threshold formula). This can be seen as follows.

The ground-state electric field is $\mathbf{E}_0 = E_0 \mathbf{e}_z$, and admissible variations are of the form

$$\mathbf{u} = u(z)\mathbf{e}_x + v(z)\mathbf{e}_y + w(z)\mathbf{e}_z, \quad \mathbf{u}(0) = \mathbf{u}(d) = \mathbf{0}.$$

The requirement $\mathbf{n}_0 \cdot \mathbf{u} = 0$ imposes a constraint on u and v , but this does not affect the analysis. In terms of these fields, the first-order change in induced polarization (23b) is given by

$$\mathbf{p}_0 = \Delta \chi^e [(\mathbf{u} \cdot \mathbf{E}_0) \mathbf{n}_0 + (\mathbf{n}_0 \cdot \mathbf{E}_0) \mathbf{u}] = \Delta \chi^e E_0 w(z) (\cos q_0 z \mathbf{e}_x + \sin q_0 z \mathbf{e}_y),$$

which implies that $\text{div } \mathbf{p}_0 = 0$ for all such admissible perturbations, and we conclude that the

magnetic approximation should apply. The switching threshold for such a twist configuration in a magnetic field was derived in [22] and is recounted in [5, Sec. 3.7]. It was assumed in [23] and other papers that the same formula but with electric parameters would give the threshold in an electric field. The validity of this magnetic-field analogy was established in subsequent analyses, including [24–26].

It is known that for larger values of q_0d the transition discussed above is preceded (at a lower field strength) by an instability to a configuration that is periodic or doubly periodic in the x - y plane—a contemporary overview of this and related issues can be found in [27]. In that case, the director perturbations \mathbf{u} would have dependencies $\mathbf{u} = \mathbf{u}(x, y, z)$, and the formula for $\text{div } \mathbf{p}_0$ would become

$$\text{div } \mathbf{p}_0 = \Delta \chi^e E_0 [w_{,x}(x, y, z) \cos q_0 z + w_{,y}(x, y, z) \sin q_0 z] \neq 0.$$

In such circumstances, the magnetic approximation would *not* apply, and the local-instability threshold in an electric field would be *elevated* compared to that predicted by the magnetic-field analogy. Periodic instabilities in planar cholesteric films are often discussed in terms of a *hydrodynamic* instability caused by what is known as the “Carr-Helfrich mechanism”—see [1, Sec. VIII.7], [2, Secs. 3.10.2 and 4.6.3], or [3, Sec. 6.3.3]. The discussion here just pertains to instabilities of dielectric origin producing equilibrium periodic orientational configurations. These are discussed, for example, in [2, Sec. 4.6.2] and [3, Sec. 6.2.2.3], and in [1, Sec. IV.2], one can indeed find the suggestion of an *elevated* electric-field threshold for the case of “strong dielectric anisotropy”—the elevating factor (based on an approximate, coarse-grained free energy) is given there to be $\sqrt{(\varepsilon_{\parallel} + \varepsilon_{\perp})/(2\varepsilon_{\perp})}$.

6.3.2. Smectic-A phases

A related periodic instability in a layered system is the Helfrich-Hurault effect in smectic-A liquid crystals [1, Sec. IV.3], [2, Sec. 5.3.3], [3, Sec. 7.1.6], [5, Sec. 6.2]. This transition involves a thin film of a smectic-A material of positive magnetic anisotropy in homeotropic alignment with layers parallel to the plane of the film and an in-plane magnetic field, which induces undulations of the layers at a critical field strength. The system was reconsidered in [28] with a *cross-plane* electric field and a material of *negative* dielectric anisotropy. The analysis in that paper indicated that the critical strength of the electric field should be strictly *greater* than that predicted by the magnetic-field analogy, by a factor of $\sqrt{\varepsilon_{\perp}/\varepsilon_{\parallel}}$ (see [28, Eqns. (25) and (30)]). We show that this is consistent with our theory.

Consider the system as depicted in Figure 4 right. The ground-state director field and electric field are given by

$$\mathbf{n}_0 = \mathbf{e}_z, \quad \mathbf{E}_0 = E_0 \mathbf{e}_z.$$

At a sufficiently strong electric field, the directors will want to distort from being parallel to \mathbf{E} (since $\varepsilon_a < 0$) causing the layers to develop a modulation in the x - y plane, with a wavelength chosen by the system. The smectic layers are modeled as level surfaces of a *layer function* f , and the liquid-crystal director is the unit normal to the layers,

$$f(x, y, z) = \text{const}, \quad \mathbf{n} = \frac{\nabla f}{|\nabla f|},$$

with the ground-state layers parallel to the x - y plane,

$$f_0 = z \Rightarrow \mathbf{n}_0 = \frac{\nabla f_0}{|\nabla f_0|} = \mathbf{e}_z.$$

If we choose the x direction for the modulation and assume that the system remains uniform

in the y direction, then the onset of undulations of the layers will take the form

$$f_\epsilon = f_0 + \epsilon g(x, z) = z + \epsilon g(x, z),$$

where g is periodic in x and vanishes at $z = 0$ and $z = d$. It follows that

$$\nabla f_\epsilon = \mathbf{e}_z + \epsilon(g_{,x}\mathbf{e}_x + g_{,z}\mathbf{e}_z) = \mathbf{n}_0 + \epsilon\mathbf{v}$$

and

$$\mathbf{n}_\epsilon = \frac{\nabla f_\epsilon}{|\nabla f_\epsilon|} = \frac{\mathbf{n}_0 + \epsilon\mathbf{v}}{|\mathbf{n}_0 + \epsilon\mathbf{v}|} = \mathbf{n}_0 + \epsilon\mathbf{u} + O(\epsilon^2), \quad \mathbf{u} = \mathbf{P}(\mathbf{n}_0)\mathbf{v} = g_{,x}\mathbf{e}_x.$$

Using these expressions for \mathbf{n}_0 , \mathbf{E}_0 , and \mathbf{u} , we obtain

$$\mathbf{p}_0 = \Delta\chi^e E_0 g_{,x}(x, z)\mathbf{e}_x \Rightarrow \operatorname{div} \mathbf{p}_0 = \Delta\chi^e E_0 g_{,xx}(x, z) \neq 0.$$

We see that the *curvature* of the undulating layers leads to a \mathbf{p}_0 that is *not* divergence free, and our test predicts an elevated instability threshold to this modulated phase, consistent with the analysis in [28]. We note that layer curvature enters the analysis of the Carr-Helfrich mechanism in a similar way [2, Sec. 4.6.3, Eqn. (4.6.32)], [3, Sec. 6.3.3, Eqns. (6.83) and (6.84)].

A similar conclusion is reached for the case of an *in-plane* electric field with a material of *positive* dielectric anisotropy (the electric-field version of the original Helfrich-Hurault instability). The only difference in this case, compared to the case discussed above, is in the orientation of the ground-state electric field. The ground-state director field, ground-state electric field, and director perturbations (associated with the onset of the layer undulations) are now given by

$$\mathbf{n}_0 = \mathbf{e}_z, \quad \mathbf{E}_0 = E_0\mathbf{e}_x, \quad \mathbf{u} = g_{,x}(x, z)\mathbf{e}_x,$$

from which we obtain

$$\mathbf{p}_0 = \Delta\chi^e E_0 g_{,x}(x, z)\mathbf{e}_z \Rightarrow \operatorname{div} \mathbf{p}_0 = \Delta\chi^e E_0 g_{,xz}(x, z) \neq 0.$$

We conclude that for this system as well, one should observe an elevation of the instability threshold compared to that predicted by the magnetic-field analogy.

6.3.3. Nematics with periodic instabilities

Nematic films are also known to develop in-plane orientational modulations under the influence of magnetic or electric fields in certain circumstances. Two examples of this are the periodic instability studied by Lonberg and Meyer in [29] and the “stripe phase” of Allender, Hornreich, and Johnson [30]. Both of these involved magnetic fields and classical Fréedericksz geometries: the splay geometry in the former case, the bend geometry in the latter. The experiment studied in [29] used a polymeric material (characterized by elastic constants with a small K_2 compared to K_1) and found that the ground-state solution became unstable at a magnetic field strength below that of the classical splay-Fréedericksz transition to a configuration that was periodic in the direction perpendicular to the plane of the ground-state director field and the applied magnetic field. The “stripe phase” in [30], on the other hand, emerged via a secondary bifurcation off the branch of classical solutions of the bend-Fréedericksz transition (at a higher magnetic field strength) at a temperature near the nematic-to-smectic-A transition (characterized by K_1 small compared to K_3). One can question if the magnetic-field analogy would be valid in either of these settings, were the experiments to be done with *electric* fields instead of magnetic fields. We show that in the former case, the answer is “yes,” while in the latter case, it is “no.”

The periodic instability of [29] is the more straightforward of the two. For this we have the splay geometry (Figure 1 left) with an equilibrium configuration that is presumed to remain uniform in x but develop a periodic modulation in y (in addition to the expected nonuniformity in the direction of the applied field, the z direction). The ground-state director field \mathbf{n}_0 , ground-state electric field \mathbf{E}_0 , and director perturbations \mathbf{u} (which must satisfy $\mathbf{n}_0 \cdot \mathbf{u} = 0$) are given by

$$\mathbf{n}_0 = \mathbf{e}_x, \quad \mathbf{E}_0 = E_0 \mathbf{e}_z, \quad \mathbf{u} = v(y, z) \mathbf{e}_y + w(y, z) \mathbf{e}_z,$$

with v and w vanishing at $z = 0$ and $z = d$. Using these in (23b), we obtain

$$\mathbf{p}_0 = \Delta \chi^e E_0 w(y, z) \mathbf{e}_x \Rightarrow \operatorname{div} \mathbf{p}_0 = 0.$$

Thus \mathbf{p}_0 is *divergence free* for all admissible director perturbations, and we conclude that the magnetic approximation should be valid: if the experiment were to be done with an electric field instead of a magnetic field, then the threshold of the instability to the modulated phase should be correctly given by the formula from the magnetic-field analogy.

The analysis of the stripe phase is a little more complicated because of the fact that it enters as a secondary bifurcation. Thus both the ground-state director field and the ground-state electric field have already been distorted by the bend-Fréedericksz transition. In the bend geometry of Figure 1 right, they would have the general forms

$$\mathbf{n}_0 = n_x^0(z) \mathbf{e}_x + n_z^0(z) \mathbf{e}_z, \quad \mathbf{E}_0 = E_0 \mathbf{e}_x + E_z(z) \mathbf{e}_z,$$

as seen in Sections 4.2 and 5. The branch that bifurcates off of this is assumed to contain equilibrium solutions that remain uniform in x but develop periodicity in y . The perturbation onto this branch would thus have the general form

$$\mathbf{u} = u(y, z) \mathbf{e}_x + v(y, z) \mathbf{e}_y + w(y, z) \mathbf{e}_z$$

and be subject to the constraints $\mathbf{n}_0 \cdot \mathbf{u} = 0$ and $\mathbf{u}(\cdot, 0) = \mathbf{u}(\cdot, d) = \mathbf{0}$. In order to conclude that the threshold for an electric-field-induced local instability should be elevated, it is sufficient to find a single perturbation \mathbf{u} such that the field \mathbf{p}_0 derived from \mathbf{n}_0 , \mathbf{E}_0 , and \mathbf{u} is *not* divergence free. For this, it is enough to consider the special case $\mathbf{u} = v(y, z) \mathbf{e}_y$, which gives

$$\mathbf{p}_0 = \Delta \chi^e [n_x^0(z) E_0 + n_z^0(z) E_z(z)] v(y, z) \mathbf{e}_y$$

and

$$\operatorname{div} \mathbf{p}_0 = \Delta \chi^e [n_x^0(z) E_0 + n_z^0(z) E_z(z)] \frac{\partial}{\partial y} v(y, z) \neq 0.$$

Thus, in contrast to the periodic instability of [29], we conclude that in the case of an electric field, the stripe-phase instability should exhibit an *elevated threshold* compared to that predicted by the magnetic-field analogy.

It is difficult to verify these predictions concerning [29] and [30], as there are no explicit formulas for the instability thresholds in either the magnetic-field or the electric-field cases for either instability. In the former case, the ground state is uniform (and known), and the instability enters with a finite period, but that period is not known a-priori—see [7, Sec. 3.3.2 and Supplementary Materials]. In the latter case, the ground state is nonuniform (and unknown), and the instability enters with an infinite period.

7. Comparison with experiment

The first experiments demonstrating a first-order transition with a static electric field in the bend geometry were reported in [11]. While the focus of that work was on the first-order nature of the transition, one can find evidence of an elevated local-instability threshold in the data provided there. The experimental setup consisted of a cell with two glass substrates separated by .5 mm and sandwiched between two stainless steel electrodes (30.0 mm x 12.5 mm x 0.5 mm) separated by 3.3 mm. This setup was chosen (in lieu of other alternatives) because it provided a fairly uniform electric field in the sample.

Several different experiments and phenomena are reported in [11]. Many of the experiments involved a combination of both an electric field and a magnetic field (differently oriented), and in addition to regular Fréedericksz transitions, instabilities to modulated phases were also observed. The data that is of use to us here is found in [11, Table II] and corresponds to a classical electric-field Fréedericksz transition in the bend geometry with no additional magnetic field. The material used was 5CB at a temperature of 33.4°C. Based upon capacitance measurements, the following hysteresis gap and first-order transition threshold (taken to be given by $V_{\text{th}} = (V_{\text{min}} + V_{\text{max}})/2$) were reported:

$$V_{\text{min}} = 4.85 \text{ V}, \quad V_{\text{th}} = 5.1 \text{ V}, \quad V_{\text{max}} = 5.35 \text{ V}. \quad (25)$$

The voltage V_{max} corresponds to the threshold at which the ground state becomes *locally unstable* (the main focus of our interest here).

In order to compare the results in this experiment with the modeling that we have discussed, we require the values of the parameters K_1 , K_3 , ε_{\parallel} , and ε_{\perp} for this material at this temperature, not all of which are given in [11]— ε_{\parallel} , ε_{\perp} , and $(K_3 - K_1)/K_3$ are given but *not* K_1 and K_3 individually. To remedy this, we have used the values for these four parameters for 5CB at $T = 33.4^\circ\text{C}$ obtained from the fitting formulas in [31]. These values are given by

$$K_1 = 3.47 \times 10^{-12} \text{ J/m}, \quad K_3 = 4.22 \times 10^{-12} \text{ J/m}, \quad \varepsilon_{\parallel} = 17.5, \quad \varepsilon_{\perp} = 7.71.$$

From these we obtain the following values for the instability threshold predicted by the magnetic-field analogy and the theoretical local-instability threshold for the outer asymptotic solution studied in Section 5:

$$V_H = \frac{\pi l}{d} \sqrt{\frac{K_3}{\varepsilon_0 \varepsilon_a}} = 4.57 \text{ V}, \quad V_{\text{max}}^{\text{theor}} = \frac{\pi l}{d} \sqrt{\frac{\varepsilon_{\parallel}}{\varepsilon_{\perp}}} \sqrt{\frac{K_3}{\varepsilon_0 \varepsilon_a}} = 6.89 \text{ V}.$$

We see that the local-instability threshold measured in the experiment (V_{max} in (25)) is indeed elevated compared to V_H , though only by roughly 17% ($(V_{\text{max}} - V_H)/V_H \doteq 0.171$), while the theoretical threshold $V_{\text{max}}^{\text{theor}}$ is elevated by roughly 51% ($(V_{\text{max}}^{\text{theor}} - V_H)/V_H \doteq 0.508$). Below we suggest some factors that could contribute to this discrepancy.

There is no formula from which to calculate the voltage of the theoretical first-order transition, and the same is true for the width of the theoretical hysteresis gap. These must be determined numerically, which we have done using the same numerical bifurcation package discussed in Section 5. Those numerical calculations produced the following values for the limit point $V_{\text{min}}^{\text{theor}}$ (the lower limit of the hysteresis gap), the first-order transition threshold $V_{\text{th}}^{\text{theor}}$ (free-energy crossover), and the bifurcation point $V_{\text{max}}^{\text{theor}}$ (the upper limit of the hysteresis gap):

$$V_{\text{min}}^{\text{theor}} = 5.99 \text{ V}, \quad V_{\text{th}}^{\text{theor}} = 6.22 \text{ V}, \quad V_{\text{max}}^{\text{theor}} = 6.89 \text{ V}.$$

By comparison, the corresponding values measured in the experiment are given in (25) above. As already noted, the ground-state local-instability thresholds V_{max} and $V_{\text{max}}^{\text{theor}}$ are elevated

from V_H by roughly 17% and 51%, while the measured and theoretical hysteresis gaps differ by

$$\Delta V = 0.5 \text{ V} \quad \text{versus} \quad \Delta V^{\text{theor}} = 0.9 \text{ V}.$$

Several factors can be mentioned as potential contributors to the facts that the instability threshold of the ground state measured in the experiment is not as elevated as theory predicts and that the hysteresis gap is not as wide as theory predicts. The formulas and numerics that have been developed here (following the original predictions in [6]) are based upon the assumption that the cell gap is small compared to the width of the cell, the asymptotic regime $0 < d/l \ll 1$. However, the cell used in the experiments reported in [11] did not have such a small aspect ratio: the actual cell dimensions were $d = 0.5 \text{ mm}$ and $l = 3.3 \text{ mm}$, giving $d/l \doteq 0.15$. For such a cell, it can be expected that the boundary influences are *not* negligible. It is also the case that the cell used in the experiments was quite thick ($500 \mu\text{m}$) in comparison with the typical thickness of cells used for experiments with liquid crystals ($10\text{--}50 \mu\text{m}$), which would lead to larger fluctuations and poorer alignment. Thus a weak-anchoring potential would probably be more realistic than the infinitely strong homeotropic anchoring assumed in our modeling, and this would be expected to lead to some reduction of the instability threshold of the ground state (from that of the strong-anchoring prediction). The large fluctuations would also tend to shrink the measured width of the hysteresis gap (the co-existence region of the ground state and the distorted director configuration), since fluctuations would drive the system to the competing solution before reaching either theoretical limit. We can say that the theory that we have discussed and the results of the experiment that we have examined are in qualitative agreement: theory predicts an elevated instability threshold for the ground state and a first-order phase transition, and both are observed in the experiment.

8. Conclusions

We have studied orientational transitions in nematic liquid crystals induced by magnetic fields and electric fields, focusing on differences between the two. These differences stem from the fact that magnetic fields can be treated as *uniform* external fields, unaffected by a liquid-crystal medium, whereas an inhomogeneous director field will cause *nonuniformity* of an electric field, in general. Because of this, magnetic-field-induced transitions are easier to analyze. The most basic instabilities of this type are the classical Fréedericksz transitions, and the widely held view is that the formula for the instability threshold for an electric-field Fréedericksz transition can be obtained from that for the magnetic-field transition in the same geometry by simply replacing the magnetic parameters by the corresponding electric parameters (the so-called “magnetic-field analogy” or “magnetic approximation”). While this is the case for the splay and twist transitions (with $\varepsilon_a > 0$), it was shown in [6] that in the case of the electric-field bend-Fréedericksz transition, the local-instability threshold should be *elevated* from that predicted by the magnetic-field analogy.

In [7] we studied the general problem of electric-field-induced instabilities in nematic systems, confirmed the results of [6], and derived necessary conditions for the local stability of general systems involving coupled director fields and electric fields. These results led to the development of a simple test for when the coupling between a director field and an electric field could lead to such an effect (altering a local-instability threshold), and they showed that the effect could only be to *elevate*, never lower, such a threshold. These results have been reviewed here, where it has been shown how the classical electric-field Fréedericksz transitions fit into the context of this more general theory.

It is natural to assume the validity of the magnetic approximation in the setting of classical Fréedericksz transitions. In all of those geometries, the ground-state director field is *uniform*; so up to the point of the instability, the electric field is uniform as well—the magnetic-field analogy is equivalent to modeling the electric field as always being uniform in the medium. In general, the electric field will develop nonuniformity *post transition*, but the natural assumption would

be that this would not affect the critical voltage at which the instability occurs. The mechanism that underlies the threshold-elevating effect is related to the mutual influence of the director field \mathbf{n} and the electric field \mathbf{E} and to changes in dielectric polarization that take place at the onset of an electric-field-induced instability ($\mathbf{P} - \mathbf{P}_0$ as a function of $\delta\mathbf{n}$). The reorientation of the director field at a configurational transition will cause changes in the induced polarization and, in general, changes in the local electric field. In certain geometries, these changes have an effect on $\text{div } \mathbf{P}$ that is *first order* in $\delta\mathbf{n}$, while in other geometries, the effect is *higher order*. First-order effects elevate instability thresholds, while higher order effects do not—they only produce quantitative differences *post transition*. We have explored these ideas in detail.

The issues are similar in spirit to flexoelectricity (polarization effects related to director distortion), but no flexoelectric coefficients are involved. The effect is purely one of induced polarization in a linear dielectric. The inclusion of flexoelectric terms in the free-energy density affects some of the analysis and leads to additional contributions to the total polarization \mathbf{P} and to the right-hand side of (23a), but these do not alter the local-instability thresholds of the classical electric-field Fréedericksz transitions, for example (see [7, Sec. 5.1]). The way in which the elevation of an instability threshold is effected can be understood from the point of view of *energetics* or from that of *torque balance*. From the *energy* point of view, the changes in the electric field that take place at the onset of such an instability increase the magnitude of the field and add to the electrostatic component of the free energy, which increases the barrier that must be overcome to destabilize the ground-state director configuration. While from the *force* point of view, the addition to the electric field caused by these changes is in the direction of the ground-state director field and therefore is *aligning* and works against the dielectric torque that is trying to rotate the ground-state director field.

Whether an electric-field Fréedericksz transition has an elevated threshold or not is not a simple matter of in-plane versus cross-plane electric field: both the bend and twist transitions have in-plane fields, yet the bend transition has an elevated threshold, while the twist transition does not. Nor is it a simple matter of whether or not nonuniformity develops in the electric field post transition: both the splay and bend transitions have nonuniform electric fields past the instability threshold, yet the bend transition has an elevated threshold, while the splay transition does not. The issue hinges on *electrostatic equilibrium* ($\text{div } \mathbf{D} = 0$, $\mathbf{D} = \varepsilon(\mathbf{n})\mathbf{E}$). If at the onset of an instability, $\text{div } \mathbf{D} = 0$ is maintained to first order in $\delta\mathbf{n}$ with an *unperturbed* ground-state electric field $\mathbf{E} = \mathbf{E}_0$, then there will *not* be an elevated threshold. If, on the other hand, a perturbation of the ground-state electric field is required to preserve $\text{div } \mathbf{D} = 0$ to first order in $\delta\mathbf{n}$, then an elevation of the local instability threshold *will* occur. The phenomenon occurs in more general systems than just classical Fréedericksz transitions.

A simple test to determine whether a transition will have an elevated local-instability threshold or not was given in Section 6.2. This test depends on the ground-state director field, the ground-state electric field, and the admissible director perturbations (all of which depend on the geometry and symmetry assumptions of the particular system). This test was applied to several electric-field-induced instabilities, including both classical and generalized Fréedericksz transitions. A few of the identified electric-field transitions that manifest this “anomalous behavior” have already been analyzed, including the bend-Fréedericksz transition with $\varepsilon_a > 0$ [6], the splay-Fréedericksz transition with $\varepsilon_a < 0$ [6], and the electric-field Helfrich-Hurault instability in smectic-A films with $\varepsilon_a < 0$ [28]. Other systems predicted by our theory and test to have elevated thresholds, but which have not yet been analyzed (to the best of our knowledge), include periodic instabilities in planar cholesteric films and the modulated “stripe phase” in nematics. The test correctly predicts that there should be *no elevation* for the thresholds of the other classical Fréedericksz transitions (splay transition with $\varepsilon_a > 0$, bend transition with $\varepsilon_a < 0$, and twist transition with $\varepsilon_a > 0$ or $\varepsilon_a < 0$), as well as for twisted nematics with a small number of twists (e.g., TNC or STN switching thresholds). It also predicts that the local-instability threshold should *not* be elevated for the periodic instability studied in [29], though this has not been analyzed either (as far as we know). We note that the test does not rely on the ground-state director field and electric field being uniform, as evidenced by the applications in Sections 6.3.1 and 6.3.3.

In summary, in certain systems the nature of the coupling between the equilibrium liquid-crystal director field and the electric field can cause an elevation of the threshold of local instability compared to that predicted by the magnetic-field analogy. We have explored this carefully and have explained why it happens and how to identify when it can happen. The effect and analysis extend beyond classical Fréedericksz transitions in nematics to other configurations (e.g., twisted nematics, secondary bifurcations in nematics), to other liquid crystal phases (e.g., cholesteric, smectic A), as well as to periodic instabilities. The analysis here was done using the macroscopic continuum theory of Oseen, Zocher, and Frank, but the development should be similar and the conclusions the same in the mesoscopic Landau-de Gennes continuum theory.

Acknowledgments

The author is grateful to O. D. Lavrentovich and P. Palffy-Muhoray for helpful discussions. Part of this work was performed at the Isaac Newton Institute for Mathematical Sciences (University of Cambridge), and the author thanks that organization for its support.

Disclosure statement

No potential conflict of interest was reported by the author.

Funding

This work was supported in part by the Division of Mathematical Sciences, U.S. National Science Foundation [grant number DMS-1211597].

ORCID

Eugene C. Gartland, Jr., <https://orcid.org/0000-0002-6956-0538>

References

- [1] S. A. Pikin. *Structural Transformations in Liquid Crystals*. Gordon and Breach Science Publishers, New York, 1991. Translated from the Russian by Michael E. Alferieff.
- [2] S. Chandrasekhar. *Liquid Crystals*. Cambridge University Press, Cambridge, 2nd edition, 1992.
- [3] Pierre Gilles de Gennes and Jacques Prost. *The Physics of Liquid Crystals*. Clarendon Press, Oxford, 2nd edition, 1993.
- [4] Epifanio G. Virga. *Variational Theories for Liquid Crystals*. Chapman & Hall, London, 1994.
- [5] Iain W. Stewart. *The Static and Dynamic Continuum Theory of Liquid Crystals*. Taylor & Francis, London, 2004.
- [6] S. M. Arakelyan, A. S. Karayan, and Yu. S. Chilingaryan. Fréedericksz transition in nematic liquid crystals in static and light fields: general features and anomalies. *Sov. Phys. Dokl.*, 29(3):202–204, 1984. Translation of Dokl. Akad. Nauk SSSR 275 (1), 52–55 (March 1984).
- [7] Eugene C. Gartland, Jr. Electric-field-induced instabilities in nematic liquid crystals. *SIAM J. Appl. Math.*, 81(2):304–334, 2021. doi: 10.1137/20M134349X.
- [8] Hans Gruler and Gerhard Meier. Electric field-induced deformations in oriented liquid crystals of the nematic type. *Mol. Cryst. Liq. Cryst.*, 16(4):299–310, 1972. doi: 10.1080/15421407208082793.

- [9] Hans Gruler, Terry J. Scheffer, and Gerhard Meier. Elastic constants of nematic liquid crystals: I. Theory of the normal deformation. *Z. Naturforsch. A*, 27(6):966–976, 1972. doi: 10.1515/zna-1972-0613.
- [10] Heinz J. Deuling. Deformation of nematic liquid crystals in an electric field. *Mol. Cryst. Liq. Cryst.*, 19(2):123–131, 1972. doi: 10.1080/15421407208083858.
- [11] B. J. Frisken and P. Palffy-Muhoray. Electric-field-induced twist and bend Freedericksz transitions in nematic liquid crystals. *Phys. Rev. A*, 39(3):1513–1518, 1989. doi: 10.1103/PhysRevA.39.1513.
- [12] B. J. Frisken and P. Palffy-Muhoray. Effects of a transverse electric field in nematics: Induced biaxiality and the bend Fréedericksz transition. *Liquid Crystals*, 5(2):623–631, 1989. doi: 10.1080/02678298908045413.
- [13] Gregory P. Richards. Numerical modeling and stability analysis of the electric-field bend-Fréedericksz transition for nematic liquid crystal cells. Masters Thesis, Applied Mathematics, Kent State University, Kent, OH, USA, August 2006.
- [14] U. D. Kini. Discontinuous orientational changes in nematics: Effects of electric and magnetic fields. *Liquid Crystals*, 8(6):745–763, 1990. doi: 10.1080/02678299008047386.
- [15] David Kinderlehrer and Biao Ou. Second variation of liquid crystal energy at $x/|x|$. *Proc. Royal Soc. Lond. A*, 437(1900):475–487, 1992. doi: 10.1098/rspa.1992.0074.
- [16] Riccardo Rosso, Epifanio G. Virga, and Samo Kralj. Local elastic stability for nematic liquid crystals. *Phys. Rev. E*, 70(1):011710, 2004. doi: 10.1103/PhysRevE.70.011710.
- [17] B. J. Frisken and P. Palffy-Muhoray. Freedericksz transitions in nematic liquid crystals: The effects of an in-plane electric field. *Phys. Rev. A*, 40(10):6099–6102, 1989. doi: 10.1103/PhysRevA.40.6099.
- [18] P. Schiller. Equilibrium structures of planar nematic and cholesteric films in electric fields. *Phase Transitions*, 29(2):59–83, 1990. doi: 10.1080/01411599008207944.
- [19] R. H. Self, C. P. Please, and T. J. Sluckin. Deformation of nematic liquid crystals in an electric field. *Eur. J. Appl. Math.*, 13:1–23, 2002. doi: 10.1017/S0956792501004740.
- [20] Gaetano Napoli. Weak anchoring effects in electrically driven Freedericksz transitions. *J. Phys. A: Math. Gen.*, 39(1):11–31, 2006. doi: 10.1088/0305-4470/39/1/002.
- [21] Ali Hasan Nayfeh. *Introduction to Perturbation Techniques*. John Wiley & Sons, New York, 1981.
- [22] F. M. Leslie. Distortion of twisted orientation patterns in liquid crystals by magnetic fields. *Mol. Cryst. Liq. Cryst.*, 12(1):57–72, 1970. doi: 10.1080/15421407008082760.
- [23] M. Schadt and W. Helfrich. Voltage-dependent optical activity of a twisted nematic liquid crystal. *Appl. Phys. Lett.*, 18(4):127–128, 1971. doi: 10.1063/1.1653593.
- [24] C. Fraser. Theoretical investigation of Fréedericksz transitions in twisted nematics with surface tilt. *J. Phys. A: Math. Gen.*, 11(7):1439–1448, 1978. doi: 10.1088/0305-4470/11/7/030.
- [25] E. P. Raynes. The theory of supertwist transitions. *Mol. Cryst. Liq. Cryst.*, 4(1):1–8, 1986. URL <https://www.tandfonline.com/doi/abs/10.1080/01406566.1986.10766872>.
- [26] P. Schiller. Perturbation theory for planar nematic twisted layers. *Liq. Cryst.*, 4(1):69–78, 1989. doi: 10.1080/02678298908028959.
- [27] Christophe Blanc, Guillaume Durey, Randall D. Kamien, Teresa Lopez-Leon, Maxim O. Lavrentovich, and Lisa Tran. Helfrich-Hurault elastic instabilities driven by geometrical frustration. *Rev. Mod. Phys.*, 95(1):015004, 2023. doi: 10.1103/RevModPhys.95.015004.
- [28] G. Bevilacqua and G. Napoli. Re-examination of the Helfrich-Hurault effect in smectic-A liquid crystals. *Phys. Rev. E*, 72(4):041708, 2005. doi: 10.1103/PhysRevE.72.041708.
- [29] Franklin Lonberg and Robert B. Meyer. New ground state for the splay-Fréedericksz transition in a polymer nematic liquid crystal. *Phys. Rev. Lett.*, 55(7):718–721, 1985. doi: 10.1103/PhysRevLett.55.718.
- [30] D. W. Allender, R. M. Hornreich, and D. L. Johnson. Theory of the stripe phase in bend-Fréedericksz-geometry nematic films. *Phys. Rev. Lett.*, 59(23):2654–2657, 1987. doi: 10.1103/PhysRevLett.59.2654.
- [31] A. Bogi and S. Faetti. Elastic, dielectric and optical constants of 4'-pentyl-4-cyanobiphenyl. *Liquid Crystals*, 28(5):729–739, 2001. doi: 10.1080/02678290010021589.